Chlorophyll-depleted wheat mutants are disturbed in photosynthetic electron flow regulation but can retain an acclimation ability to a fluctuating light regime

Lorenzo Ferroni (Conceptualization) (Investigation) (Formal analysis) (Writing - original draft) (Writing - review and editing) (Supervision), Marek Živčak (Conceptualization) (Formal analysis) (Data curation) (Writing - review and editing), Oksana Sytar (Investigation) (Formal analysis) (Writing - original draft), Marek Kovár (Software) (Investigation) (Formal analysis) (Data curation), Nobuyoshi Watanabe (Resources), Simonetta Pancaldi (Investigation) (Formal analysis), Costanza Baldisserotto (Investigation) (Formal analysis), Marián Brestič (Conceptualization) (Writing - review and editing) (Supervision) (Funding acquisition)

PII: S0098-8472(20)30182-9

DOI: https://doi.org/10.1016/j.envexpbot.2020.104156

Reference: EEB 104156

To appear in: *Environmental and Experimental Botany*

Received Date: 12 February 2020

Revised Date: 13 May 2020

Accepted Date: 11 June 2020

Please cite this article as: Ferroni L, Živčak M, Sytar O, Kovár M, Watanabe N, Pancaldi S, Baldisserotto C, Brestič M, Chlorophyll-depleted wheat mutants are disturbed in photosynthetic electron flow regulation but can retain an acclimation ability to a fluctuating light regime, *Environmental and Experimental Botany* (2020), doi: https://doi.org/10.1016/j.envexpbot.2020.104156

Chlorophyll-depleted wheat mutants are disturbed in photosynthetic electron flow regulation but can retain an acclimation ability to a fluctuating light regime

Lorenzo Ferroni[a,b], Marek Živčak[b], Oksana Sytar[b], Marek Kovár[b], Nobuyoshi Watanabe[c], Simonetta Pancaldi[a], Costanza Baldisserotto[a], Marián Brestič[b,d]

[a] Laboratory of Plant Cytophysiology, Department of Life Sciences and Biotechnology, University of Ferrara, Ferrara, Italy

[b] Department of Plant Physiology, Slovak University of Agriculture, Nitra, Slovakia

[c] College of Agriculture, Ibaraki University, Inashiki, Ibaraki, Japan

[d] Department of Botany and Plant Physiology, Faculty of Agrobiology, Food and Natural Resources, Czech University of Life Sciences, Prague, Czech Republic

Co-corresponding Authors:

Lorenzo Ferroni

Department of Life Sciences and Biotechnology, University of Ferrara, C.so Ercole I d'Este 32, 44121 Ferrara, Italy

Phone: +39 0532 293785

Email: lorenzo.ferroni@unife.it

Marek Živčak

Department of Plant Physiology, Slovak University of Agriculture, Nitra, A. Hlinku 2, 94976 Nitra, Slovak Republic

Phone: +421 37 641 4821

Email: marek.zivcak@uniag.sk

Oksana Sytar

Department of Plant Physiology, Slovak University of Agriculture, Nitra, A. Hlinku 2, 94976 Nitra, Slovak Republic

Phone: +421 37 641 4979

Email: oksana.sytar@uniag.sk

HIGHLIGHTS

- A disturbance in photosynthetic electron flow affects the chlorophyll-depleted wheat mutants.
- Unexpectedly long-term acclimation to light fluctuations can be allowed in mutants.
- Successful development of a fluctuating-light phenotype depends on the mutated locus.
- Compensation of the mutation involves use of alternative electron sinks and thylakoid structural re-organization.

ABSTRACT

The search for more productive crops is exploring accessions with reduced chlorophyll accumulation in leaves, which would promote plant growth mainly because of a higher light transmittance throughout the canopy. Under continuous light, chlorophyll-depleted *chlorina* mutants of wheat can reach yields similar to WT; however, their performance under fluctuating light could possibly be lowered by a disturbed photosynthetic electron transport.

Six *chlorina* mutants of *Triticum aestivum* (ANBW4A, ANBW4B, ANK32A) or *T. durum* (ANDW7A, ANDW7B, ANDW8A) were compared to WT genotypes under continuous and fluctuating light regimes, the latter obtained through a randomized pattern of light intensity changes. After two weeks of plant acclimation under either regimes, light energy management was thoroughly analysed for four weeks.

All *chlorina* mutants showed a defective ability to regulate the electron poise during a fast rise in irradiance. Different extent of deregulation depended on mutation and genomic background, durum

wheat being more severely impaired than bread wheat. However, a great acclimative capacity to a fluctuating light regime unexpectedly still characterized the *chlorina* wheat plants, with the only exception of the mutants carrying the *cn-B1b* mutated locus (ANDW7B and ANBW4B). Under fluctuating light, all other *chlorina* mutants developed indeed an ability to improve their control of electron transport against the recurrent reducing bursts caused by lightflecks. Compensatory responses included the regulation of energy distribution between photosystems, the use of alternative electron sinks, and a structural reorganization of the thylakoid system. However, in no case a reduced chlorophyll content led to more productive plants. Among 23 measured photosynthetic parameters, especially the non-regulatory energy dissipation in photosystem II - *Y(NO) –*, when probed during a light rise, can be proposed in automated phenotyping experiments as a straightforward index to be used for *chlorina* wheat screening with respect to potential productivity.

KEYWORDS

Wheat, chlorina mutant, fluctuating light, photosynthetic electron transport, photosynthetic acclimation

Abbreviations: α_{II}, relative light absorption by PSII as compared to incident PAR; ν_H^+, proton flux; τECS, time constant of the ECS decay; *A*, assimilation; CEF, cyclic electron flow; Chl, chlorophyll; CL, continuous light; *dII*, energy distribution to PSII; DAS, days after sowing; ET, electron transport; ECS, electrochromic shift; ECS_{st}, rise in 520 nm absorbance induced by a single-turnover flash; F_0 and F_0', minimum chlorophyll fluorescence in the dark- or light-acclimated state, respectively; F_M, F_M' and F_M'' maximum chlorophyll fluorescence in the dark- or light-acclimated or dark-relaxed state, respectively; F_V, variable chlorophyll fluorescence; FL, fluctuating light; g_H^+, proton conductance; J_A, electron flow to alternative sinks; J_G, electron flow to photosynthesis and photorespiration; J_{PSII}, total linear electron flow; LHCII, light-harvesting complex II; *NPQ*, non-photochemical quenching; PAR, photosynthetically active

radiation; P_M and P_M', maximum P700 signal in the dark- or light-acclimated state; *P*, P700 absorbance at a given light intensity; PSII, photosystem II; *pmf*, proton motive force; *1-qP*, fraction of reduced Q_A quinone; RLC, rapid light curve; SP, saturation pulse; SPPU, Slovak PlantScreen™ Phenotyping Unit; *Y(CO₂)*, quantum yield of CO_2 assimilation; *Y(NA)*, *Y(ND)*, *Y(PSI)* quantum yields of dissipation in acceptor-limited or donor-limited PSI, and of PSI photochemistry, respectively; *Y(NO)*, *Y(NPQ)*, *Y(PSII)* quantum yields of non-regulatory energy dissipation, regulatory energy dissipation, and PSII photochemistry, respectively; *Y(qI)*, quantum yield of photoinhibited PSII.

1. INTRODUCTION

Because of its outstanding importance worldwide, an increase in the productivity of wheat has always been a desirable target, explored through the selection of new genotypes. A renewed interest regards the so-called yellow-green *chlorina* mutants, which are characterized by a lowered chlorophyll (Chl) content as compared to recurrent wild-type (WT) genotypes. In general, the *chlorina* phenotypes of wheat are generated by recessive mutations at *cn* loci mapping to chromosomes 7, leading to a partial deficiency of Chl synthesis. The candidates for the defect are subunits of the magnesium chelatase, which catalyses Mg^{2+} insertion into protoporphyrin IX (Falbel *et al.,* 1996; Koval, 1997; Watanabe and Koval, 2003; Kosuge *et al.,* 2011; Wang *et al.,* 2018; Jiang *et al.,* 2019). The rationale for investigating such mutants resides on the idea that the Chl content of wheat leaves would be unnecessarily high as compared to the real energy needs for carbon fixation (e.g. Jin *et al.,* 2016; Wang *et al.,* 2018). Moreover, in a dense crop cultivation, the apical leaves shade the lower ones, suggesting that a reduced Chl accumulation in leaves would promote plant growth because of a higher light transmittance throughout the canopy (Song *et al.,* 2017; Friedland *et al.,* 2019). Even recently a reduction of Photosystem II (PSII) antenna size obtained in a *chlorina* mutant was reported to improve wheat

productivity (Wang *et al.,* 2018), but other evidence suggests that in general this is not the case. In fact, typical wheat *chlorina* mutants are stress sensitive and have a very low yield capacity under field conditions. To increase their productivity, mutations were transferred from donors into the genome of some major crops with greater productivity. In the resulting genotypes, growth and productivity were more developed in spite of Chl depletion (Watanabe and Koval, 2003). For instance, the phenotype of near-isogenic ANK hexaploid lines of bread wheat is quite well characterized, including some molecular and biochemical properties (Watanabe and Koval, 2003; Rassadina *et al.,* 2005; Kosuge *et al.,* 2011). The *chlorina* phenotype, which occurs in their early growth phases, tends to re-establish at least partly to WT during plant growth (Brestič *et al.,* 2015, 2016). Nonetheless, a recent comparative analysis of wheat *chlorina* mutants showed a great variability in such a behaviour. In particular, the severity of the *chlorina* phenotype was higher when plants were cultivated outdoor than in a growth chamber, and this result was attributed to an improper regulation of the photosynthetic electron transport (ET; Živčak *et al.,* 2019). In fact, a limited ability to prevent the over-reduction of photosystem I (PSI) acceptor side makes PSI more prone to inactivation and, if not adequately counteracted, can even be lethal for plants (Shimakawa and Miyake, 2018a). There is ever-accumulating evidence about the importance of a well-regulated photosystem antenna complement to specifically preserve the integrity of photosystems under fluctuating light (FL) regimes (Grieco *et al.,* 2012; Tikkanen *et al.,* 2012; Brestič *et al.,* 2015). Accordingly, among the several factors impacting on the outdoor cultivation of wheat, natural fluctuations in light intensity were proposed to play a primary role in determining the (in)success of *chlorina* mutants (Živčak *et al.,* 2019).

Response of photosynthesis to fluctuations in irradiance with time constants up to the range of tens of minutes is a current major scientific problem addressed in its different facets, from molecular mechanisms to whole plant phenotyping (Kaiser *et al.,* 2018a; van Bezouw *et al.,* 2019). The regulation of photosynthesis under conditions of constant/continuous light (CL) is supported by an ideal balance

between light-use efficiency and photoprotection (Kaiser *et al.,* 2018a; Matthews *et al.,* 2018). Conversely, under FL, plants cope with an incessant challenge to the regulation of photosynthesis. Consequently, successful plant growth depends on the promptness of the dynamic regulation of the photosynthetic apparatus, assuming that the faster the response to the change, the less will be the loss of efficiency (Edwards *et al.,* 2012). At the level of the photosynthetic membrane, the regulation of light use efficiency is strongly linked to the dynamism of the antenna complement of photosystems. In particular, light-harvesting complex II (LHCII) regulates energy distribution between PSI and PSII (Wientjes *et al.,* 2013; Grieco *et al.,* 2015; Ferroni *et al.,* 2016), contributes quenching sites for the safe thermal dissipation of excess absorbed energy (Ruban, 2016; Nicol *et al.,* 2019), and is involved in other regulatory mechanisms, such as PSII connectivity (Živčak *et al.,* 2014; Albanese *et al.,* 2017) and PSII-to-PSI energy spillover (Yokono *et al.,* 2015; Ferroni *et al.,* 2018). Moreover, it is involved in the grana-intergrana differentiation of the thylakoid membranes, which relates to the so-called *lateral heterogeneity* of PSI and PSII distribution (Anderson, 2012).

Since wheat *chlorina* mutants are impaired in Chl *a* and Chl *b* synthesis, they are disturbed in the assembly of the LHC complement (Falbel *et al.,* 1996). Based on the central role of LHCs in the regulation of the thylakoid membrane, it is conceivable that *chlorina* mutants experience an altered ET. But to what extent do natural FL influence the mutant growth in the absence of other environmental stresses? And also, can growth impairments be linked to ET disturbance under FL? Our work aims at contributing an answer to such questions using a set of six *chlorina* mutants, of either bread (ANBW4A, ANBW4B, ANK32A) or durum wheat (ANDW7A, ANDW7B, ANDW8A), with different performance as compared to their recurrent WT genotypes (NS67 and LD222, respectively) (Živčak *et al.*, 2019). In two cases (ANBW4A/ANDW7A; ANBW4B/ANDW7B), the same mutation is present in both species of wheat, thus allowing a phenotype comparison between the hexaploid bread wheat vs tetraploid durum wheat. In the last years, the effect of FL on photosynthesis and growth was mainly studied under “rectangular”

artificial fluctuations, alternating low and high irradiance (Suorsa *et al.,* 2012; Yamori, 2016). In a variant, a FL regime was obtained by applying periodic 20 s-long lightflecks (Kaiser *et al.,* 2018b). Vialet-Chabrand *et al.* (2017) introduced a fixed pattern of a naturally FL regime, simulating a relatively clear day. Subsequently, Matthews *et al.* (2018) elaborated an artificial light regime based on a sinusoidal variation with a randomized pattern of light alterations, while keeping a constant daily light intensity. Such an approach closely simulates a natural light environment, in which plants are exposed every day to a unique pattern of irradiance (Kaiser *et al.,* 2018b; Slattery *et al.,* 2018; Tanaka *et al.,* 2019). For our experiment, a similar protocol of randomized FL intensity was specifically developed in the Slovak PlantScreen™ Phenotyping Unit (SPPU), a phenotyping facility of the European Plant Phenotyping Network EPPN^{2020} (Fig. 1; Supplementary Fig. 1).

The results here reported are part of a more comprehensive automated phenotyping experiment with wheat *chlorina* mutants. In order to allow a critical interpretation of the automated phenotyping data, it was deemed vital to first validate the FL regime protocol at SPPU using independent and well-established manual measurements of photosynthetic traits. Therefore, in this report we focus on the (de)regulation of the photosynthetic electron poise in wheat *chlorina* mutants in relation to carbon assimilation and chloroplast ultrastructure, in particular testing a potential negative effect of growth under a randomized FL regime. Our results demonstrate that the protocol set up at SPPU allows for an effective categorisation of wheat *chlorina* mutants based on their specific sensitivity to FL.

[FIGURE 1 – 1 column fitting]

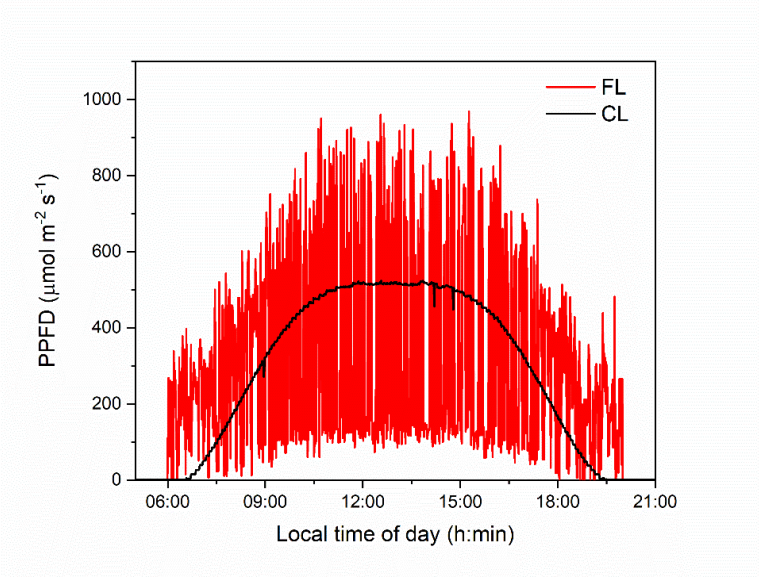

Fig. 1. Diurnal light regimes in the continuous light (CL) and fluctuating light (FL) sectors of the Slovak PlantScreen™ Phenotyping Unit growth chamber. Areas under the curves correspond to the same light energy of ca. 16 mol photons m^{-2} day^{-1}. Irradiance measurements are exemplified from data collected by sensor 3 (CL) and sensor 4 (FL).

2. MATERIAL AND METHODS

2.1. Plant cultivation facility

The plant cultivation was set up at the SPPU (Agrobiotech Centre of the Slovak University of Agriculture in Nitra, Slovak Republic). In the growth room, the photoperiod was 14:10 h (day:night), temperature was 27:22°C (day:night) and relative humidity 50:65% (day:night). Control of water level in pots (70% soil-water content) was performed by the automated watering system of SPPU every second day. For the experiment on contrasting light regimes, the growth room was divided into two sectors with a black curtain to avoid any cross influence between contrasting lights (Supplementary Fig. 1). Moreover, the transparent roof of the installation at Agrobiotech Centre was covered with a black cloth, almost completely screening the external sunlight (<2-3 µmol photons m^{-2} s^{-1}). Using dimmerable custom LED

bars system with cool white lights (Photon Systems Instruments, Drasov, Czech Republic), irradiance in the non-fluctuating, CL sector was set at ca. 500 μmol photons m^{-2} s^{-1} of photosynthetically active radiation (PAR), which simulated a moderately bright day without direct sunlight. Steady-state irradiance was gradually reached through an increasing ramp in the morning (sunrise simulation) and decreased likewise in the late afternoon (sunset simulation). In the FL sector, the light fluctuations were controlled by the software "Light Control" specifically developed by Photon Systems Instruments. In particular, light oscillated between ca. 100 and 1000 μmol photons m^{-2} s^{-1}, without a fixed period, but following a random algorithm, which modified the light intensity within the two extremes in a time scale of few minutes. Similar to CL sector, extent of light oscillations in FL sector followed the increasing and decreasing light ramps for sunrise and sunset. Overall, the FL sector simulated cloudy days in the open field with frequent sunflecks filtering through the clouds (Kaiser *et al.,* 2018a). The FL regime was fine-tuned to provide plants with approximately the same amount of photons on a daily basis as the plants grown under CL (daily light integral, ca. 16 mol photons m^{-2} day^{-1}; Fig. 1). In both sectors, irradiance was monitored using fixed quantum-radiometer probes (Photon Systems Instruments) at the level of plants. Beside light intensity, environmental monitoring also included temperature and relative humidity, as exemplified in Supplementary Fig. 1.

2.2. Plant material, experimental design and data treatment

For the experiments, the following lines of wheat were used: (1) bread wheat, *Triticum aestivum* L.: Chl-less mutant lines ANBW4A, ANBW4B, ANK32A, and the recurrent WT cv. Novosibirskaya 67, NS67; (2) durum wheat, *Triticum durum* L.: Chl-less mutant lines ANDW7A, ANDW7B, ANDW8A, and the recurrent WT cv. LD222. The details on genotypes used in the experiments are reported in Table 1.

Genotype	Mutated locus	Chromosome	Donor

Triticum aestivum	NS 67 (WT)	-	-	
	ANBW-4A	*cn-A1d*	7AL	CDd6 mutant of *T. durum* Langdon
	ANBW-4B	*cn-B1b*	7BL	CDd2 mutant of *T. durum* Langdon
	ANK-32A	*cn-A1a*	7AL	Chlorina mutant of *T. aestivum* "CS"
Triticum durum	LD 222 (WT)	-	-	-
	ANDW-7A	*cn-A1d*	7AL	CDd6 mutant of *T. durum* Langdon
	ANDW-7B	*cn-B1b*	7BL	CDd2 mutant of *T. durum* Langdon
	ANDW-8A	Unknown	Unknown	Light green mutant of *T. durum*

Table 1 Information on the genetic background of the wheat mutant lines used in the experiment

Seeds were sown in pots containing 930 g Klasmann TS 3 soil (containing: 140 mg L^{-1} N, 160 mg L^{-1} P_2O_5, 180 mg L^{-1} K_2O, 100 mg L^{-1} Mg, EDTA-chelated Fe, trace elements, pH(H_2O) 6.0; Klasmann-Deilmann GmbH, Geeste, Germany) and germinated in greenhouse in June 2018. After germination, pots with seedlings were transferred to the phenotyping unit, registered into the system software (PlantScreen™ Server, Photon System Instruments) with bar codes, and randomly positioned on the belts. Plants were distributed in five belts (two for CL, three for FL), each containing 18 pots with one plant. Each genotype was represented with 4-7 replicates for total 90 plants (Supplementary Fig. 1G). In both sectors, plant positions were routinely randomized twice per week to avoid any possible margin effect. During two weeks, plants were allowed to grow under the two contrasting light regimes and were monitored by automated phenotyping routines (not reported in this paper). Around 35 days after sowing (DAS), all plants had developed their fourth leaf, which had a sufficient size and solidity to allow measurements with each device described in the following sections without any relevant mechanical

stress. Results obtained ca. 35, 42, 49 and 55 DAS are indicated in terms of week 1, 2, 3 and 4, respectively.

Once per week, leaf chlorophyll content of all plants was analysed with a non-destructive Chl meter SPAD-502 (Konica-Minolta, Osaka, Japan). A general evaluation of plant performance was obtained 13 weeks after sowing in terms of aboveground plant dry weight biomass.

For the more time-consuming determinations of photosynthetic properties with Dual-PAM, JTS-100 and Licor 6400, one plant for each of 16 combinations (8 genotypes × 2 light regimes) was analysed every week. Week after week and for each instrumental test, the plant used for analysis was never the same; therefore, the time course of parameters was obtained from independent plants and trends were checked by linear regression, using CL and FL data as separate or combined sets. Although each data point was obtained from an individual plant, a statistical data treatment was still possible and two-way ANOVA was run to look for significant effects of variables “genotype” and “light treatment” (and their interaction). Considering that, as expected, the plants tended to approach stable values, analysis of pooled data (all weeks or 2-4-week subset) was chosen for a convenient representation of results. Post-hoc analysis of differences was run with Tukey’s test. However, complete information on data points is made available as supplementary materials. Statistical analyses, including fitting tests, were run with Origin version 2019b (OriginLab Corporation, Northampton, MA, USA) and significant differences were examined with α=0.05.

2.3. Simultaneous analysis of chlorophyll fluorescence and P700 redox state

Photochemical responses of PSI and PSII were analysed simultaneously with a Dual-PAM-100 (Walz, Germany) endowed with a chlorophyll fluorescence unit and a P700 dual wavelength (830/875 nm) unit. Measurement of parameters was obtained using the saturation pulse (SP) method according to Klughammer and Schreiber (1994). SPs of 0.5 s were applied at an irradiance of 10.000 µmol photons m^{-2}

s^{-1}. The measuring routine was modified from Živčak *et al.* (2019) and schematically illustrated in Supplementary Fig. 2**.** Whole plants taken from the growth facility were dark-acclimated for 15 min in a dark box and for ca. 2 min in the measuring head of Dual-PAM. After the determination of F_0, F_M and P_M, the leaf was exposed to a low intensity actinic light (134 µmol photons m^{-2} s^{-1}) to start the photosynthetic processes until a steady-state was reached, as assessed applying a SP every 30 s. Subsequently, a rapid light curve (RLC; Kalaji et al. 2014) was triggered with 30-s-long steps from 14 to 1960 µmol photons m^{-2} s^{-1}; after each light intensity, a SP followed by far-red pulse for F_0' determination was fired. The dynamic regulation of ET was analysed sampling the parameters measured at 539 and 1960 µmol photons m^{-2} s^{-1} during the RLC. At the end of the RLC, the leaf was exposed to 7 min light at 1602 µmol photons m^{-2} s^{-1} to analyse the steady-state parameters under high light, with SPs applied every 30 s. Finally, the relaxation of parameters was recorded in darkness for 20 min. Each measurement took collectively ca. one hour.

The values used for calculation of PSII-related parameters were: F, F' — fluorescence emission from dark- or light-acclimated leaf, respectively; F_0, F_0' — minimum fluorescence in the dark-acclimated (open PSII centres) or light-acclimated state (closed PSII centres), respectively; F_M, F_M', F_M'' — maximum fluorescence emitted by dark-acclimated, light-acclimated or dark-relaxed leaves, respectively. These values were combined to calculate: the maximum quantum yield of PSII photochemistry $F_V/F_M=(F_M-F_0)/F_M$; the actual quantum yield of PSII photochemistry $Y(PSII)=(F_M'-F')/F_M'$ (Genty *et al.,* 1989); the quantum yield of the non-regulatory dissipation as heat and fluorescence $Y(NO)=F'/F_M$ (Hendrickson *et al.,* 2004); the quantum yield of the regulatory thermal dissipation $Y(NPQ)$=1-$Y(PSII)$-$Y(NO)$ (Hendrickson *et al.,* 2004); the non-photochemical quenching of chlorophyll fluorescence $NPQ=Y(NPQ)/Y(NO)=(F_M-F_M')/F_M'$; the redox poise of the primary electron acceptor Q_A of PSII, $Q_A^-/[Q_A$ total], $1-qP = 1-[(F_M'-F')/(F_M'-F_0')]$; the quantum yield of energy dissipation in photoinhibited PSII

centres $Y(qI) = F_V/F_M – F_V''/F_M''$, where F_V'' and F_M'' were evaluated at the end of the 20 min-long dark relaxation.

The measured values for PSI-related parameters were: P – P700 absorbance at a given light intensity; P_M, P_M' — maximum P700 signal measured using a SP following a short far-red pre-illumination in the dark- or light-acclimated state, respectively. The P700 parameters were used to calculate PSI quantum yields as follows (Klughammer and Schreiber, 1994): effective quantum efficiency of PSI photochemistry at a given PAR, $Y(PSI)=(P_M' – P)/P_M$; oxidation status of PSI donor side, i.e., the fraction of P700 oxidized at given state, $P700^+$/(P700 total), $Y(ND)=P/P_M$; reduction status of PSI acceptor side, i.e., the fraction of overall P700 oxidized in a given state by SP due to a lack of electron acceptors, $Y(NA)=(P_M – P_M')/P_M$.

The fraction of energy absorbed by PSII (*dII*) was calculated according to Sukhov *et al.* (2015). In particular, considering that, at low light, plants have minimum cyclic electron flow (CEF; Huang *et al.,* 2012), the electron flow through PSI approximately equals the electron flow through PSII. Therefore, the *Y(PSI)* and *Y(PSII)* values obtained during rapid light curves at 78 µmol photons m^{-2} s^{-1} were used in the following equation:

$$dII = \frac{1}{\frac{Y(PSII)}{Y(PSI)} + 1}$$

2.4. Analysis of electrochromic shift

The electrochromic shift (ECS) is a change of the absorption spectra of some carotenoids caused by the generation of an electrochemical ΔpH across the thylakoid membrane, therefore it provides a means to quantify the photosynthetic proton motive force (*pmf*), as reviewed by Bailleul *et al.* (2010). ECS was measured with a JTS-100 spectrometer (BioLogic Science Instruments, Seyssinet-Pariset, France). Before ECS measurements, a rapid rise in 520 nm absorbance (ECS_{st}) was induced in the leaf by a saturating

single-turnover flash. After ECS_{st} evaluation, the LED control of the spectrometer was set to irradiate the leaf with an actinic light close to average growth irradiance, provided by orange LEDs (493 µmol photons m^{-2} s^{-1}). Based on preliminary Dual-PAM analyses, steady-state of ∆pH was assumed to be reached after 10 min light exposure; subsequently, light was turned off and the relaxation kinetics of the carotenoid electrochromic band shift was measured at 520 nm. The ECS signal at 520 nm was normalized against the ECS_{st} previously obtained to account for differences in leaf thickness and chlorophyll content between leaves (Takizawa *et al.,* 2007). The rapid decay (within 150 ms) of the normalized ECS signal during the dark pulse was fit with an exponential decay function using Origin version 2019b (OriginLab Corporation, Northampton, MA, USA). The *pmf* between light and dark was estimated from the amplitude of the rapid decay. Since the time constant of the relaxation (τECS) is inversely proportional to the proton conductivity (g_{H^+}) of the thylakoid membrane through the ATP synthase, g_{H^+} was determined as the inverse of the decay time constant [τECS^{-1}] (Sacksteder and Kramer, 2000; Huang *et al.,* 2018). The relative light-driven proton flux was calculated as $\nu_{H^+}=pmf \times g_{H^+}$ (Huang *et al.*, 2018).

2.5. Simultaneous analysis of gas exchange and chlorophyll fluorescence

An open infrared gas exchange system Licor 6400 (Licor, USA), equipped with a fluorescence unit, was used to measure the photosynthetic rate and, at the same time, the Chl emission using the SP method. The conditions within the measuring head were set to be similar to those in the growth room: a leaf temperature of 25 °C, reference CO_2 of 400 µL L^{-1}, ambient air humidity (manually checked between 50-70%). The light source was a red LED light unit supplemented with 10% blue LED light to facilitate stomata opening.

The measuring protocol was adapted from Živčak *et al.* (2019). After a short dark acclimation (<3 min) inside the measuring chamber for approximation of F_V/F_M, the leaf was exposed to 4 min light at 400 µmol photons m^{-2} s^{-1} and then 4 min at 800 µmol photons m^{-2} s^{-1} to activate the Calvin-Benson-

Bassham cycle and induce full opening of stomata. Subsequently, a sequence of nine decreasing light intensities was triggered from 1600 to 25 µmol photons m^{-2} s^{-1}, followed by a further step in darkness. Each step lasted for ca. 4 min to reach a steady state and each final record of gas exchange was associated with application of a SP for *Y(PSII)* determination through Chl fluorescence. Each measurement took collectively ca. one hour. *Y(PSII)* was used to calculate the linear ET, J_{PSII}=*Y(PSII)* × Irradiance × α_{II} (Krall and Edwards, 1992), where α_{II} is the product of the light absorption by the leaf and the fraction of energy absorbed by PSII. The J_{PSII} value directly provided by Licor software in the hypothesis of equal distribution of energy between PSI and PSII was corrected using the *dII* factor calculated from Dual-PAM data.

Light curves of carbon assimilation (*A*) were fitted with a non-rectangular hyperbola (http://landflux.org) to calculate the apparent quantum yield of CO_2 fixation [$Y(CO_2)$]. Using the *A* values obtained at 500 µmol photons m^{-2} s^{-1}, i.e. similar to the average irradiance of growth, the total amount of ET J_g required for Rubisco activity was calculated according to Harley *et al.* (1992):

$$J_g = \frac{(A + Rd)(4Ci + 4\frac{\Gamma^*}{\alpha})}{Ci - \Gamma^*}$$

where *Ci* is the measured value of intercellular CO_2 concentration, *Γ** is the photosynthetic CO_2 compensation point in the absence of dark respiration (37 µmol mol^{-1} at 25°C; Bernacchi *et al.,* 2002), and α=0.5 is the ratio of CO_2 release per RuBisCO oxygenation. The day respiration *Rd* was approximated as the dark respiration reduced by 0.65 factor, based on values measured by Yin *et al.* (2009) for wheat. The electron flux to alternative sinks was calculated as J_A=J_{PSII}–J_g according to Živčak *et al.* (2013).

2.6. Transmission electron microscopy

For electron microscopy, at the middle of photoperiod a small piece was cut from the central portion of the leaf blade excluding the central vein and further reduced to smaller samples of ca. 4 mm^2. After

rinsing with 0.1 M K-Na phosphate buffer at 4°C, the samples were fixed with 3% glutaraldehyde in the same buffer for 4 h at 4°C (Ferroni *et al.,* 2016). Subsequently, samples were rinsed twice with buffer and sent to the Electron Microscopy Centre of the University of Ferrara for further processing. After 2 h post-fixation with OsO_4 1% at room temperature, samples were dehydrated in an ascending acetone series and embedded in Durcupan ACM resin according to routine protocols. Ultrathin sections were contrasted with uranyl acetate and lead citrate, and finally observed with a Hitachi H800 transmission electron microscope (Hitachi, Tokio, Japan).

3. RESULTS

3.1. Only ANDW4B and ANDW7B are specifically impaired by a FL regime

During the four weeks of monitoring, the bread and durum wheat plants showed an increase in Chl content, though to a different extent (Fig. 2A, D). Apart from the most relevant Chl depletion in ANK32A, *chlorina* phenotype was generally more severe in durum than in bread wheat. Chl content recovered to WT values in ANBW4A and ANBW4B mutants of bread wheat, but not in the corresponding ANDW7A and ANDW7B of durum wheat. A specific exacerbation of the chlorina phenotype by FL occurred only in mutants carrying *cn-B1b* locus, ANDW7B and ANBW4B, although the latter progressively recovered to values similar to CL counterpart. The negative effect of *cn-B1b* on the acclimation to FL emerged also as lower final shoot biomass in ANDW7B and ANBW4B (Fig. 2B, E). Effect of *cn-A1d* mutation was not consistent between bread (ANBW4A) and durum wheat (ANDW7A). Finally, ANK32A and ANDW8A did not show any specific influence of FL on biomass. Correlation between Chl content and final shoot biomass was obvious in durum wheat across all genotypes (linear model weighted on standard deviations, Adjusted $R^2 = 0.96$, $P<10^{-4}$). Bread wheat was instead distributed into two point clouds, ANK32A *vs* all other genotypes. In particular, ANBW4B achieved a lower final biomass of under FL in spite of the recovered Chl content (Fig. 2C, F).

Fig. 3A-B shows average values of CO_2 assimilation (*A*) over four weeks, while the corresponding time courses are reported in Supplementary Fig. 3A-F. In both bread and durum wheat, *chlorina* mutations influenced steady-state *A* at low light, rather than at saturating or average growth light, and confirmed especially the lower photosynthetic capacity of ANK32A and ANDW7B (Table 2). A specific effect on *A* at low irradiance is an expected consequence of decreased yields of CO_2 fixation $Y(CO_2)$, which occurred indeed in all mutants and matched well their biomass accumulation (Fig. 3C, Table 2, Supplementary Fig. 3G-K). Durum wheat was overall more severely impaired than bread wheat, with an additional and strong negative effect of the FL regime in ANDW7B (Table 2, Fig. 3C).

[FIGURE 2 – 2 column fitting]

[FIGURE 3 – 1.5 column fitting]

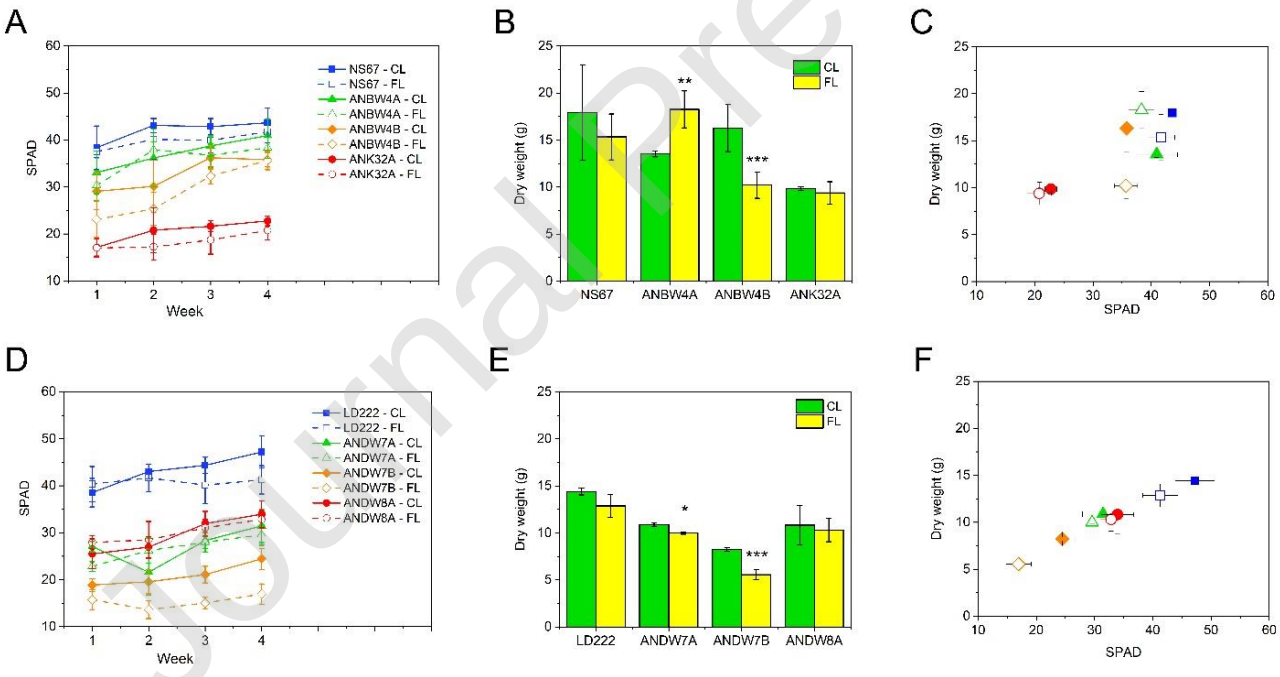

Fig. 2. Chlorophyll content and aboveground biomass accumulation in chlorina mutants of wheat grown under continuous (CL; A-C) or fluctuating (FL; D-F) light.

(A,D) Variation in chlorophyll content as SPAD-502 values over a period of four weeks (see text for details); each point is mean of 4-7 measurements with SE.

(B,E) Final aboveground dry biomass at the 13th week after sowing; each point is mean of 2-3 plants with SE and asterisks indicate significant differences between CL an FL plants.

(C,F) Covariation of final aboveground dry biomass and SPAD values.

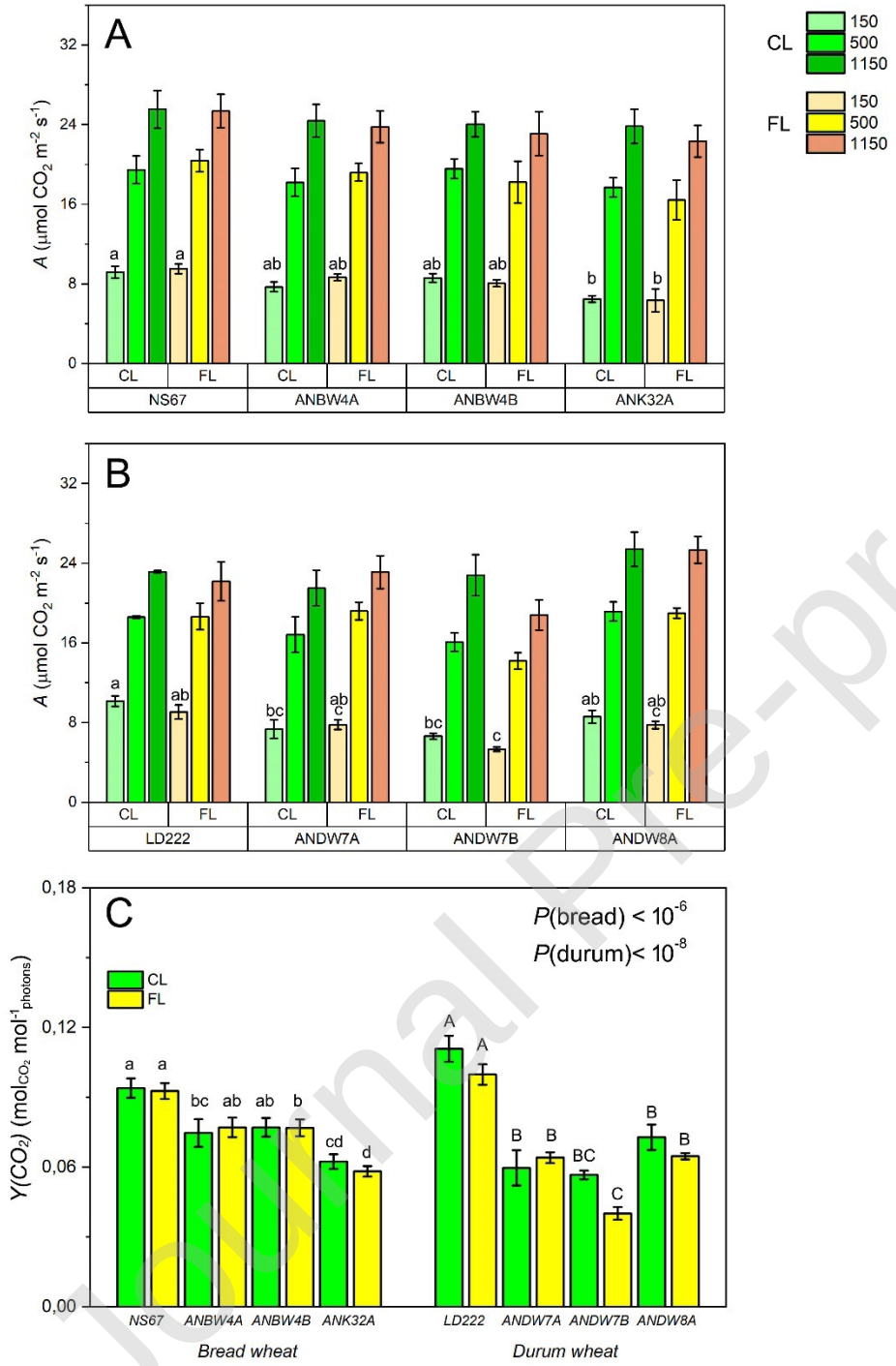

Fig. 3. CO_2 fixation in *chlorina* mutants of wheat grown under continuous (CL) or fluctuating (FL) light.

(A, B) CO_2 assimilation (*A*) at three irradiance values, representative of low light (e.g., minimum in FL), steady-state growth light, and high light (e.g., irradiance peaks in FL) in bread wheat (A) and durum wheat (B).

(C) Quantum yield of CO_2 fixation, $Y(CO_2)$.

All values are means with SE of 4 measurements from independent plants sampled at four subsequent weeks. In C, the resulting probability from ANOVA is reported for bread and durum wheat. When $P<0.05$, a post-hoc Tukey's test was run and results are reported in graphs (different letters mean statistically significant difference). In view of statistical inference reported in Table 2, in panels A and B the significant differences are reported only for *A* at low light values.

	Parameter	**Factor "light"**	**Factor "mutant"**	**Interaction**	**Selected paired t-test CL vs FL**	**Significant trends**
Triticum aestivum	$\boldsymbol{A_{150}}$	0.71	**$<10^{-3}$** (ANK32A)	0.61	ANBW4A (FL>CL, <0.05)	↑ ANBW4A (all, <0.05) ↑ ANBW4B (FL, <0.05)
	$\boldsymbol{A_{500}}$	0.86	0.28	0.74	---	↑ NS67 (FL, <0.01) ↑ ANBW4A (CL, <0.05) ↑ ANBW4B (FL, <0.01) ↑ ANK32A (CL, <0.05)
	$\boldsymbol{A_{1150}}$	0.51	0.55	0.98	ANK32A (FL<CL, <0.05)	↑ ALL (all, <0.01)
	$\boldsymbol{Y(CO_2)}$	0.81	**$<10^{-8}$** (ANK32A, ANBW4A, ANBW4B)	0.51	---	None
Triticum durum	$\boldsymbol{A_{150}}$	0.10	**$<10^{-4}$** (ANDW7A, ANDW7B)	0.43	ANDW7B (FL<CL, <0.05)	↑ ANDW7A (CL, <0.05)
	$\boldsymbol{A_{500}}$	0.96	**<0.01** (ANDW7B)	0.34	ANDW7B (FL<CL, <0.05)	↑ ANDW7A (CL, <0.05) ↑ ANDW7B (all, <0.05)
	$\boldsymbol{A_{1150}}$	0.46	0.07	0.39	ANDW7B (FL<CL, <0.05)	↑ LD222 (FL, $<10^{-3}$) ↑ ANDW7B (FL, <0.05)
	$\boldsymbol{Y(CO_2)}$	**<0.05**	**$<10^{-10}$** (ANDW7A, ANDW7B; ANDW8A)	0.24	ANDW7B (FL<CL, <0.01)	↑ ANDW7A (CL, <0.01)

Table 2 Results of statistical analyses on parameters related to CO_2 fixation in bread and durum wheat grown under continuous (CL) or fluctuating (FL) light. A_{150}, A_{500}, A_{1150} represent steady-state net assimilation at 150, 500 and 1150 µmol photons m^{-2} s^{-1}, respectively; $Y(CO_2)$ is the quantum yield of CO_2 fixation (mol CO_2 mol^{-1} photons).

For each parameter, data obtained during 4 weeks were analysed with two-way ANOVA (factor "light", factor "mutant" and their interaction). When factor "mutant" was significant, data from mutants were further analysed with Tukey's test. Resulting *P* values are reported; significant effect of factors is highlighted in bold. Only when at the origin of variability there was a significant difference between mutant and respective WT, the mutant(s) is reported in brackets.

Paired Student's *t*-test was run to check difference between FL and CL for individual mutants.

Trends were analysed with linear regression; significant increasing or decreasing trends are indicated with ↑ and ↓, respectively, and it is also indicated when the trend regarded both data sets (all) or only CL/FL.

3.2. PSI and PSII parameters at the steady state reveal the detrimental effect of growth under FL on ANDW7B, but not on ANBW4B

The reduced performance of *chlorina* mutants was hypothesised to depend on an altered energy flow from light harvesting to utilization, which could possibly be further exacerbated by growth under FL. To check the regulation of photosynthetic light reactions, we analysed many photosynthetic parameters related to PSII and PSI activity. Results of statistical analyses on the 4-weeks data sets are summarized in Table 3 for bread wheat and Table 4 for durum wheat. However, for the sake of better readability and

considering that the values tended to stabilize, in the following paragraphs we refer to mean values over the period of weeks 2-4.

In both WT cultivars, F_V/F_M was constant during the experiment, while increasing trends characterized ANK32A and the durum wheat mutants (Supplementary Fig. 4A-B). However, F_V/F_M obtained from mutants were similar to those of the respective WT and in the range of an optimal PSII photochemical activity (Fig. 4A). Similar to F_V/F_M, the PSII complementary yields probed under steady-state high light were not informative about major defects in regulation, except in ANDW7B, which was impaired in keeping the plastoquinone pool oxidized, i.e. higher *Y(NO)*, while it reduced *Y(NPQ)* (Fig. 4B-D; Supplementary Fig. 4E-H). In bread wheat significant global ANOVA for *Y(NPQ)* depended on a difference between the extremes, highest in ANBW4B and lowest in ANK32A, neither of them being yet different from NS67 (Fig. 4D; Table 3; Supplementary Fig. 4G).

The specific amount of photo-oxidizable PSI was analysed normalizing P_M against the corresponding Chl content as SPAD values. P_M/SPAD was generally increasing during the experiment, especially in bread wheat, but no effect of mutations or light regime could be revealed (Fig. 4E; Supplementary Fig. 5A-B). Under high light at the steady state, *Y(PSI)* was not much informative as well, apart from an evident progressive recovery in ANK32A (Fig. 4F; Supplementary Fig. 5C-D; Table 3). Major changes regarded instead the limitation of PSI at its acceptor or donor side. To protect PSI, *Y(NA)* should be kept as low as possible by removing fluently electrons from PSI; at the same time, plants are also expected to promote the safe accumulation of oxidized PSI centres ($P700^+$), whose relative amount is meant by *Y(ND)* (Shimakawa and Miyake, 2018b). Altered *Y(NA)* and *Y(ND)* indicated a significant disturbance in the regulation of the steady-state ET not only in ANDW7B – as seen also with *Y(NO)* – but also in ANK32A and, to a lesser extent, ANDW7A. Yet, no specific effect of the light regime was observed (**Fig. 4G-H**; **Supplementary Fig. 5E-H**; **Tables 3-4**).

A trait previously reported to characterize the wheat *chlorina* mutants is a low PSI-to-PSII quantum yield ratio, *Y(PSI)/Y(PSII)* (Živčak *et al.,* 2019). This was confirmed in ANK32A among bread wheat mutants and in all durum wheat mutants, but only ANDW7B showed a tendency to even lower values under FL (Fig. 5A; Supplementary Fig. 6). The simplest interpretation of a lower *Y(PSI)/Y(PSII)* is a decrease in CEF, whose main expected effect is a lower ∆pH across the thylakoid membrane and, consequently, a lower induction of *NPQ* (Munekage *et al.,* 2002). Interestingly, only ANDW7B under FL experienced a decrease in *Y(NPQ)* (Fig. 5A; Fig. 4D; Table 4; Supplementary Fig. 6B). However, beside CEF, the steady-state *Y(NPQ)* clearly depends also on the parallel H^+ efflux through the ATP synthase. We analysed mutants about their capacity to generate and use the proton motive force (*pmf*) across the thylakoid membrane for ATP synthesis (H^+ conductance, g_{H^+}) in leaves acclimated to average growth light. In durum wheat, the *pmf* results were in good agreement with *Y(PSI)/Y(PSII)*, thus confirming a lower CEF capacity in mutants. Specifically in ANDW7B when grown under FL, the marked decrease in *pmf* was also helped by a tendency to higher g_{H^+}. Among bread wheat mutants, *pmf* was halved in ANK32A, but its g_{H^+} was specifically emphasized only under FL (Fig. 5B-C; Supplementary Fig. 6; Table 4). The membrane regulation was further analysed in terms of total proton flux v_{H^+}. All mutants varied within, or at least close, to the corresponding WT v_{H^+} ranges, testifying to a sufficient ability of the *chlorina* mutants to sustain ATP synthesis (Fig. 5D; Supplementary Fig. 6G-H). Nevertheless, in ANBW4B v_{H^+} was consistently lower when grown under FL in comparison to CL, though converging to WT value at the 4th week (Table 4).

In summary, besides the visibly disturbed ANK32A, the parameters related to the steady-state activity of photosystems revealed the higher severity of ANDW7B phenotype under FL. Conversely, the mutant of bread wheat carrying the same mutation, ANBW4B, did not show comparable major alterations that may justify its markedly lower performance under FL, but only a lower total proton flux, which however progressively improved.

[FIGURE 4 – 2 column fitting]

[FIGURE 5 – 2 column fitting]

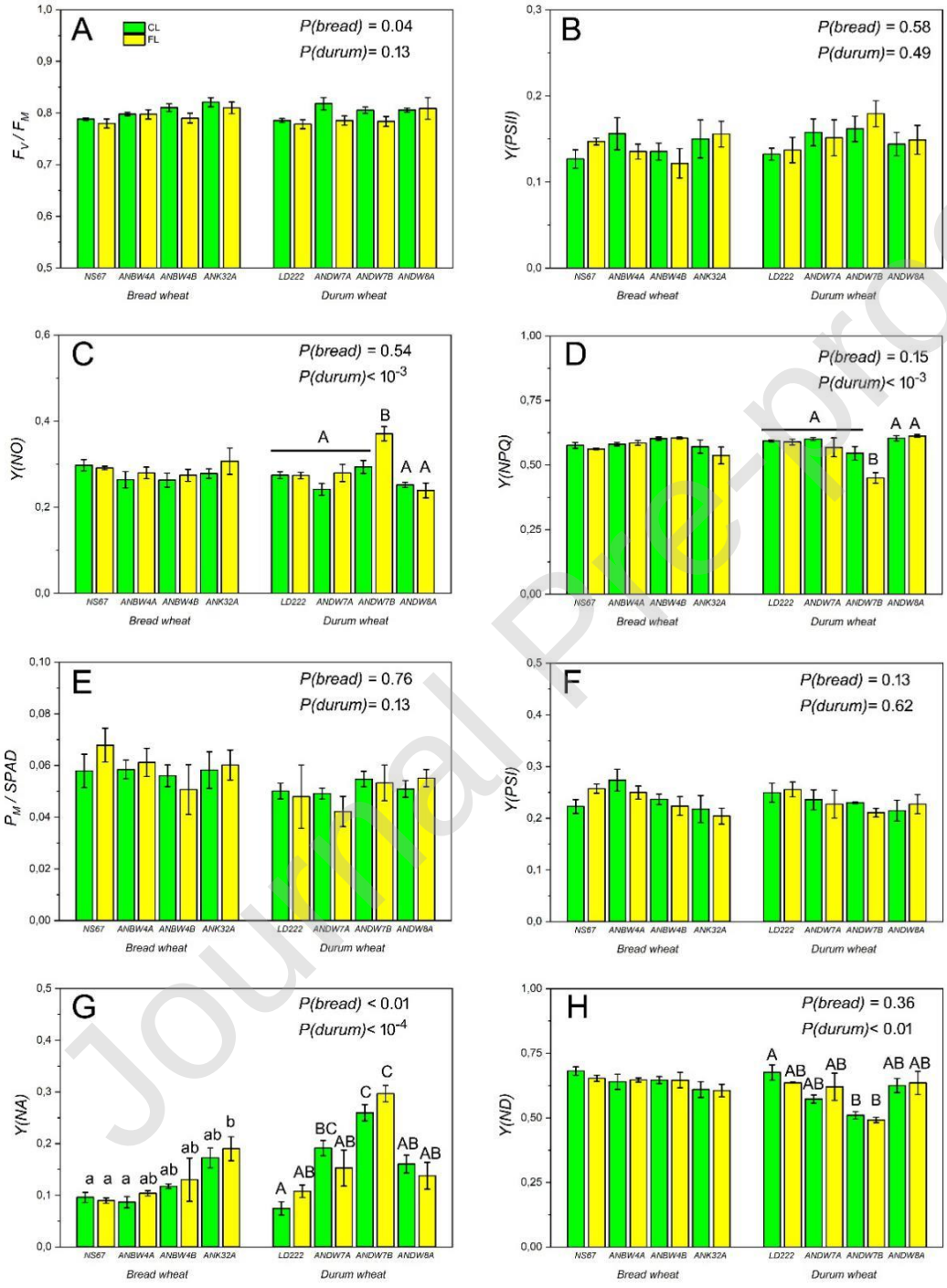

Fig. 4. Parameters related to Photosystem II (PSII) and Photosystem I (PSI) activity under high light at the steady state in *chlorina* mutants of wheat grown under continuous (CL) or fluctuating (FL) light.

(A) Maximum quantum yield of PSII, F_V/F_M.

(B-D) Quantum yields of PSII photochemistry *Y(PSII)*, non-regulatory energy dissipation *Y(NO)*, regulatory energy dissipation *Y(NPQ)*.

(E) Maximum photo-oxidizable PSI normalized to the specific leaf chlorophyll content as SPAD, $P_M/SPAD$.

(F-H) Quantum yields of PSI photochemistry *Y(PSI)*, energy dissipation in acceptor-limited PSI *Y(NA)* or in donor-limited PSI *Y(ND)*.

Values are means with SE of 3 measurements from independent plants sampled at three subsequent weeks, as describe in the text. Data were analysed with one-way ANOVA separately for bread and durum wheat, resulting probability is reported in each graph. When $P<0.05$, a post-hoc Tukey's test was run and results are reported in graphs (different letters mean statistically significant difference). In the case of panel A with F_V/F_M, the results of post-hoc test are not reported because limited to a difference between the two extremes (N67-FL *vs* ANK32A-CL).

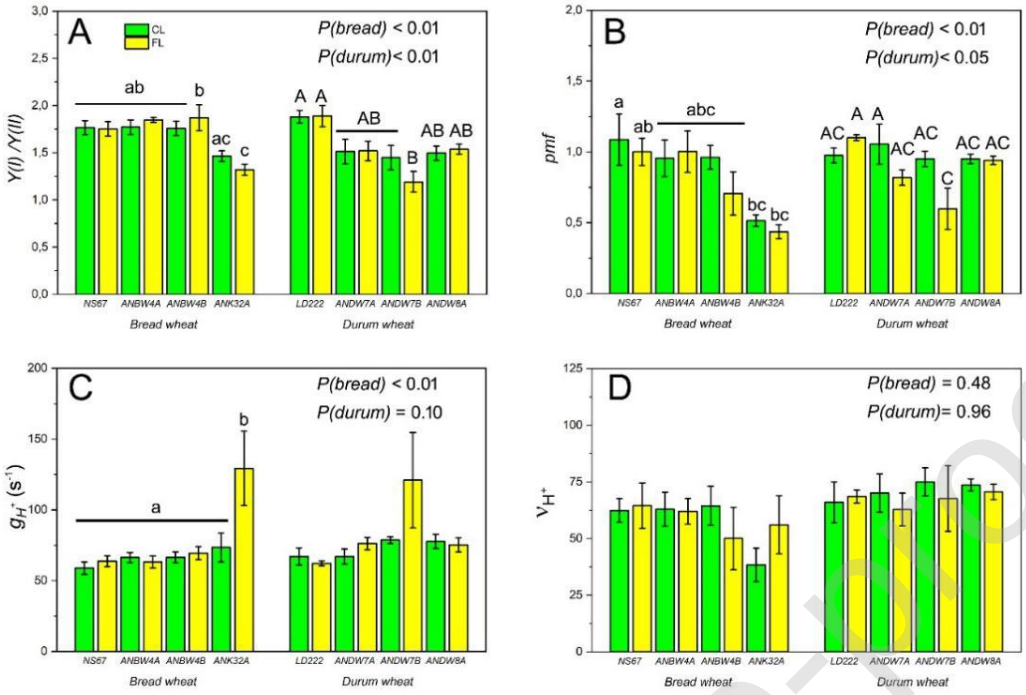

Fig. 5. Parameters related to the generation and use of the trans-thylakoidal proton motive force in *chlorina* mutants of wheat grown under continuous (CL) or fluctuating (FL) light.

(A) Quantum yield ratio between PSI and PSII photochemical yields, *Y(I)/Y(II)*, calculated from Dual-PAM measurements.

(B-D) Proton motive force *pmf*, proton conductance g_H^+ and total proton flux v_H^+ obtained from electrochromic shift analysis using a JTS-100 spectrometer.

Values are means with SE of 3 measurements from independent plants sampled at three subsequent weeks, as describe in the text. Data were analysed with one-way ANOVA separately for bread and durum wheat, resulting probability is reported in each graph. When $P<0.05$, a post-hoc Tukey's test was run and results are reported in graphs (different letters mean statistically significant difference).

Parameter	Factor "light"	Factor "mutant"	Interaction	Selected paired t-test CL vs FL	Significant trends
F_V/F_M	0.69	0.34	0.85	---	↑ ANK32A (all, <0.01)
Y(II)	0.92	0.49	0.45	---	None
Y(NO)	0.42	0.21	0.46	---	↓ANBW4A (all, <0.05) ↓ANK32A (all, <0.01)
Y(NPQ)	0.32	**<0.01**	0.49	---	None
NPQ	0.32	0.06	0.94	---	↑ANBW4A (all, <0.05) ↑ANK32A (all, <0.05)
Δ*Y(NO)*	0.75	**<10^{-6}** (ANK32A, ANBW4B)	0.37	---	↓ ANBW4B (FL, <0.01) ↓ ANK32A (FL, <0.05)
Δ*(1-qP)*	0.38	0.14	0.94	---	None
P_M/SPAD	0.78	0.83	0.88	---	↑ All
Y(I)	0.91	**<0.05**	0.78	---	↑ANBW4A (all, <0.05) ↑ANK32A (all, <0.01)
Y(ND)	0.68	**<0.01** (ANK32A)	0.77	---	↓ ANBW4A (all, <0.05)
Y(NA)	0.78	**<10^{-3}** (ANK32A)	0.88	---	↓ ANK32A (all, <0.05)
Δ*Y(NA)*	0.23	**<0.01** (ANK32A)	**<0.05** (ANK32A-CL)	NS67 (FL<CL, <0.05) ANK32A (FL<CL, =0.06)	↓ ANBW4B (FL, <0.01) ↓ ANK32A (FL, <0.05)
Y(I)/Y(II)	0.34	**<10^{-5}** (ANK32A)	0.34	---	None
Y(qI)	0.74	0.13	0.77	---	↓ANBW4A (all, <0.05) ↓ANK32A (all, <0.01)
dII	0.08	**<10^{-6}** (ANK32A)	**<0.05** (ANBW4B-FL)	ANBW4B (FL>CL, <0.05)	None
pmf	0.17	**<10^{-3}** (ANK32A, ANBW4B)	0.77	ANBW4B (FL<CL, =0.05)	↑ANBW4A (FL, <0.05) ↑ANBW4B (FL, <0.05)
g_H^+	0.42	**<0.01** (ANK32A)	0.39	---	(↓ANK32A FL, P=0.06)
v_H^+	0.41	0.18	0.52	ANBW4B (FL<CL, <0.05)	↑ ANDW4B (all, <0.05)

Table 3 Results of statistical analyses on parameters related to PSI and PSII activity in bread wheat grown under continuous (CL) or fluctuating (FL) light.

For details about statistics, refer to legend of **Table 2**.

Parameter	Factor "light"	Factor "mutant"	Interaction	Selected paired t-test CL vs FL	Significant trends
F_V/F_M	0.14	0.72	0.76	ANDW7A (FL<CL, <0.05)	↑ ANDW7A (all, <0.05) ↑ ANDW7B (all, <0.05) ↑ ANDW8A (all, <0.01)
Y(II)	0.84	0.14	0.89	---	None
Y(NO)	0.05	**<0.01** (ANDW7B)	0.17	ANDW7B (FL<CL, <0.01)	↓ LD222 (all, $<10^{-3}$) ↓ ANDW7A (CL, <0.01) ↓ ANDW7B (FL, <0.05) ↓ ANDW8A (all, $<10^{-3}$)
Y(NPQ)	**<0.05** (FL<CL)	**$<10^{-5}$** (ANDW7B)	**<0.05** (ANDW7B CL-FL)	ANDW7B (FL<CL, <0.05)	↑ ANDW8A (all, <0.05)
NPQ	0.10	**$<10^{-3}$** (ANDW7A, ANDW7B, ANDW8A)	0.19	ANDW7B (FL<CL, <0.05)	↑ LD222 (CL, <0.05) ↑ ANDW7A (CL, <0.05) ↑ ANDW7B (FL, <0.05) ↑ ANDW8A (all, <0.05)
ΔY(NO)	0.53	**$<10^{-9}$** (ANDW7A, ANDW7B, ANDW8A)	0.28	ANDW7B (FL>CL, <0.05)	↓ ANDW7B (FL, <0.05) ↓ ANDW8A (all, 0.06)
Δ(1-qP)	0.68	**$<10^{-3}$** (ANDW7A, ANDW7B)	0.83	---	↓ ANDW7B (FL, <0.05)
P_M/SPAD	0.54	0.95	0.93	---	↑ ANDW7B (all, <0.05) ↑ ANDW8A (all, <0.01)
Y(I)	0.91	0.17	0.91	---	↑ LD222 (all, <0.05) ↑ ANDW8A (all, <0.05)
Y(ND)	0.99	**$<10^{-4}$** (ANDW7A, ANDW7B)	0.53	---	none
Y(NA)	0.93	**$<10^{-4}$** (ANDW7A, ANDW7B)	0.75	---	None
ΔY(NA)	0.30	**$<10^{-4}$** (ANDW7A, ANDW7B, ANDW8A)	0.24	---	None
Y(I)/Y(II)	0.64	**$<10^{-4}$** (ANDW7A, ANDW7B, ANDW8A)	0.92	---	None
Y(qI)	0.40	0.21	0.70	---	↓ ANDW8A (all, <0.05)
dII	**<0.05** (FL>CL)	**<0.05** (ANDW7B)	0.12	ANDW7A (FL>CL, <0.05)	↑ LD222 (all, <0.05)

pmf	0.07	0.10	0.29	---	None
g_H^+	0.26	**<0.05** (ANDW7B)	0.51		None
ν_H^+	0.37	0.70	0.86	---	↑ ANDW8A (all, <0.05)

Table 4 Results of statistical analyses on parameters related to PSI and PSII activity in durum wheat grown under continuous (CL) or fluctuating (FL) light.

For details about statistics, refer to legend of **Table 2**.

3.3. *Chlorina* mutants, ANBW4B included, are compromised in the control of the electron poise upon an upward fluctuation in irradiance

The effectiveness of ET regulation upon a sudden increase in irradiance was analysed using *Y(NO)* and *Y(NA)*. In fact, during a minutes-scale rise from moderate to very high light (539 to 1960 μmol photons m^{-2} s^{-1}, sampled from RLC), a well-regulated system is expected to ensure a fluent ET, keeping $\Delta Y(NO)$ and $\Delta Y(NA)$ as close as possible to zero. Comparative results in bread and durum wheat are reported in Fig. 6A-B and trends in Supplementary Fig. 7.

In bread wheat, the hypothesis of close-to-zero $\Delta Y(NO)$ upon a rapid light ramp was indeed verified in NS67, but also in ANBW4A; on the contrary, the capacity of prompt oxidation of the ET chain was very reduced in ANK32A, and a similar tendency occurred also in ANBW4B (Fig. 6A; Table 3; Supplementary Fig. 7). Results about $\Delta Y(NA)$ were overall similar to $\Delta Y(NO)$, but with an evident exception in ANK32A (Fig. 6B; Table 3). In fact, ANK32A was highly defective in keeping $\Delta Y(NA)$ low when grown in CL, but not in FL. Despite statistically non-significant in the averaged results of Fig. 6B, a tendency to higher $\Delta Y(NA)$ occurred in ANBW4B under FL as well, because of an early very strong defect in ET regulation, which was steadily relieved during four weeks (Table 3; Supplementary Fig. 7). All

durum wheat *chlorina* mutants suffered to some extent from a disturbance of the electron poise upon a lightfleck. This was obvious from $\Delta Y(NO)$, but also from $\Delta Y(NA)$; overall, there was an increase in deregulation severity as ANDW8A<ANDW7A<ANDW7B (Fig. 6B).

The covariation of $\Delta Y(NA)$ and $\Delta Y(NO)$ in Fig. 6C shows that the minimum $\Delta Y(NA)$ and even negative $\Delta Y(NO)$ characterized the WT cultivars acclimated to FL, testifying to their excellent ability to control the ET. The $\Delta Y(NA)$-$\Delta Y(NO)$ correlation was very significant, especially excluding the outlier point ANK32A-FL (linear regression, *Adjusted* R^2=0.81, $P<10^{-5}$); therefore, an inferior capacity of final acceptors to receive electrons flowing out of PSI was generally accompanied by an increment in plastoquinone reduction. However, ANK32A and, to a lesser extent, ANDW7A actually improved their control of $\Delta Y(NA)$ - but not of $\Delta Y(NO)$ – when acclimated to FL regime.

To assess the excitation energy pressure inside PSII we examined *1-qP*, which normalizes the electron traffic on the PSII population that can trap electrons, i.e. excludes PSII centres quenched by *NPQ*; moreover, it depends on the whole of mechanisms that consume electrons (Björkman and Demmig-Adams, 1995; Kalaji *et al.,* 2017). Activation of the latter mechanisms during a light ramp should indeed minimize ΔY(*1-qP*). In spite of the defects highlighted on the photosynthetic ET, bread wheat mutants succeeded in controlling ΔY(*1-qP*) as compared to NS67 (Fig. 6D; Supplementary Fig. 7). Not the same in durum wheat: global two-way ANOVA indicated a very significant effect of mutation on ΔY(*1-qP*) because of higher values in ANDW7A (P<0.01) and ANDW7B ($P<10^{-3}$) (Table 4). Because of a convergence of mutants to WT values, ANOVA on data collected during weeks 2-4 indicated only a marginal significance, easily attributable to ANDW7A and ANDW7B (Fig. 6D; Supplementary Fig. 7). The expected consequence of a higher energy pressure inside PSII is PSII photoinhibition, which occurred specifically in ANDW7B (Fig. 6E; Supplementary Fig. 7).

In summary, a short-term light increase caused a deregulation of the electron poise to a different extent depending on *chlorina* mutant, from quasi-WT conditions (ANBW4A) to strong impairment (ANK32A, ANDW7B). In addition, ANBW4B, which was negligibly affected under high light at the steady state, actually revealed a tendency to defective oxidation of the ET chain during a rapid light ramp, although the defect was limited to the plants grown in a FL regime and slowly reversing to a WT condition.

[FIGURE 6 – 2 column fitting]

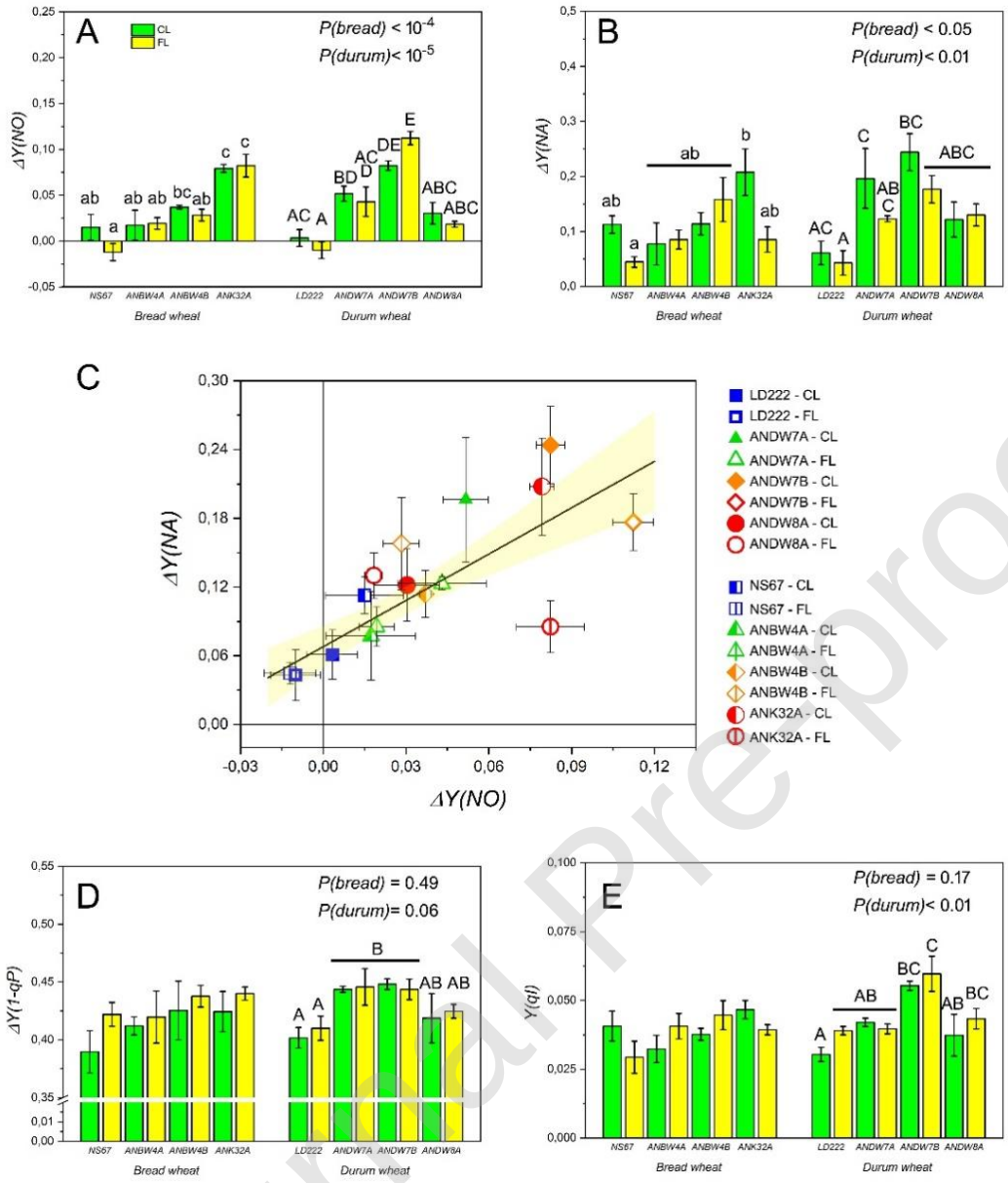

Fig. 6. Parameters related to the dynamic regulation of photosynthesis in *chlorina* mutants of wheat grown under continuous (CL) or fluctuating (FL) light.

(A-B) *ΔY(NO)* and *ΔY(NA)* are the difference in the respective parameters (non-regulatory energy dissipation in PSII, energy dissipation in acceptor-limited PSI, respectively), measured during a minutes-scale rise from growth light (539 μmol photons m^{-2} s^{-1}) to high light (1960 μmol photons m^{-2} s^{-1}).

(C) Covariation of *ΔY(NO)* and *ΔY(NA)*; the solid line and the light yellow band represent a weighted linear regression with confidence bands at 98%, respectively; calculation excludes the outlier point ANK32A-FL.

(D) *Δ(1-qP)* is the difference in excitation energy pressure inside PSII calculated during a light rise as in (A-B).

(E) *Y(qI)* is PSII photoinhibition at the end of the Dual-PAM measuring routine, that is after a rapid light curve followed by a steady-state exposure to high light.

All values are means with SE of 3 measurements from independent plants sampled at three subsequent weeks, as describe in the text. Data in all histograms were analysed with one-way ANOVA separately for bread and durum wheat, resulting probability is reported in each graph. When $P<0.05$ (or global two-ANOVA as in Table 4 yielded $P<0.05$ in case of panel D), a post-hoc Tukey's test was run and results are reported in graphs (different letters mean statistically significant difference).

3.4. Deregulated electron poise can occur in aberrant or normal thylakoid architectures

In the hypothesis of an insufficient ET regulation in *chlorina* mutants, we analysed which thylakoid architectures can be permissive or not to a proper control of the photosynthetic electron flow. Comparative views of representative chloroplasts in WT and mutant leaves are shown in Fig. 7 and selected details in Supplementary Fig. 8. Both WT had a typical grana-intergrana organization of the thylakoid system. Especially in FL-grown plants, in close connection with the thylakoids some small sparse osmiophilic plastoglobules were observed (Fig. 7A, E, I, M). The presence of primary starch grains was common in LD222, not in NS67.

In bread wheat mutants, the thylakoid architecture ranged from nearly WT to strongly altered (Fig. 7A-H). In both ANBW4A and ANBW4B, the overall abundance of the thylakoid system was not

different from that of NS67, albeit grana were smaller especially under FL. However, the most obvious alteration in ANBW4B was the conspicuous accumulation of plastoglobule clusters interspersed among thylakoids (Fig. 7G). A strong general reduction of the membrane system affected instead ANK32A. Beside small grana, especially under FL the most characteristic feature of ANK32A were long arrays of single straight and parallel thylakoids, originating from large grana (Fig. 7D, H). The transition from stacked to non-appressed thylakoid domains was very neat, giving rise to a remarkably regular structure (Supplementary Fig. 8B).

A generalized reduction of the thylakoid system affected all durum wheat mutants, further exacerbated by a FL regime in ANDW8A and ANDW7B (Fig. 7I-P; Supplementary Fig. 8D). The least severe condition occurred in ANDW7A, though with an evident accumulation of plastoglobule clusters (Supplementary Fig. 8E). Some aberrations were observed in ANDW8A, where prevailing small grana were accompanied by arrays of single thylakoids sometimes connected with large grana, analogous to those in ANK32A, though often smaller or less ordered (Fig. 7L, P; Supplementary Fig. 8C-D). Plastoglobules were also easily observed. In ANDW7B, the chloroplast ultrastructure was profoundly disturbed specifically under FL (Fig. 7O). The visibly reduced thylakoid system lost its ordered organization, showing in the same organelle very small grana, some arrays of single thylakoids (Supplementary Fig. 8F) and, distinctively, frequent thylakoid doublets, i.e. long lamellae formed by only two appressed thylakoids (Supplementary Fig. 8G).

Collectively, in *chlorina* mutants the thylakoid system was not merely reduced, but also structurally disturbed at different levels of severity, depending on mutant and light regime. The most aberrant membrane organization was found in the two *chlorina* mutants affected by the strongest alterations in ET regulation and emphasized under FL: ANK32A and ANDW7B. However, interestingly, intermediate levels of severity in ET deregulation occurred in either an altered (ANDW8A) or nearly normal (ANBW4B) thylakoid organization.

[FIGURE 7 – 2 column fitting]

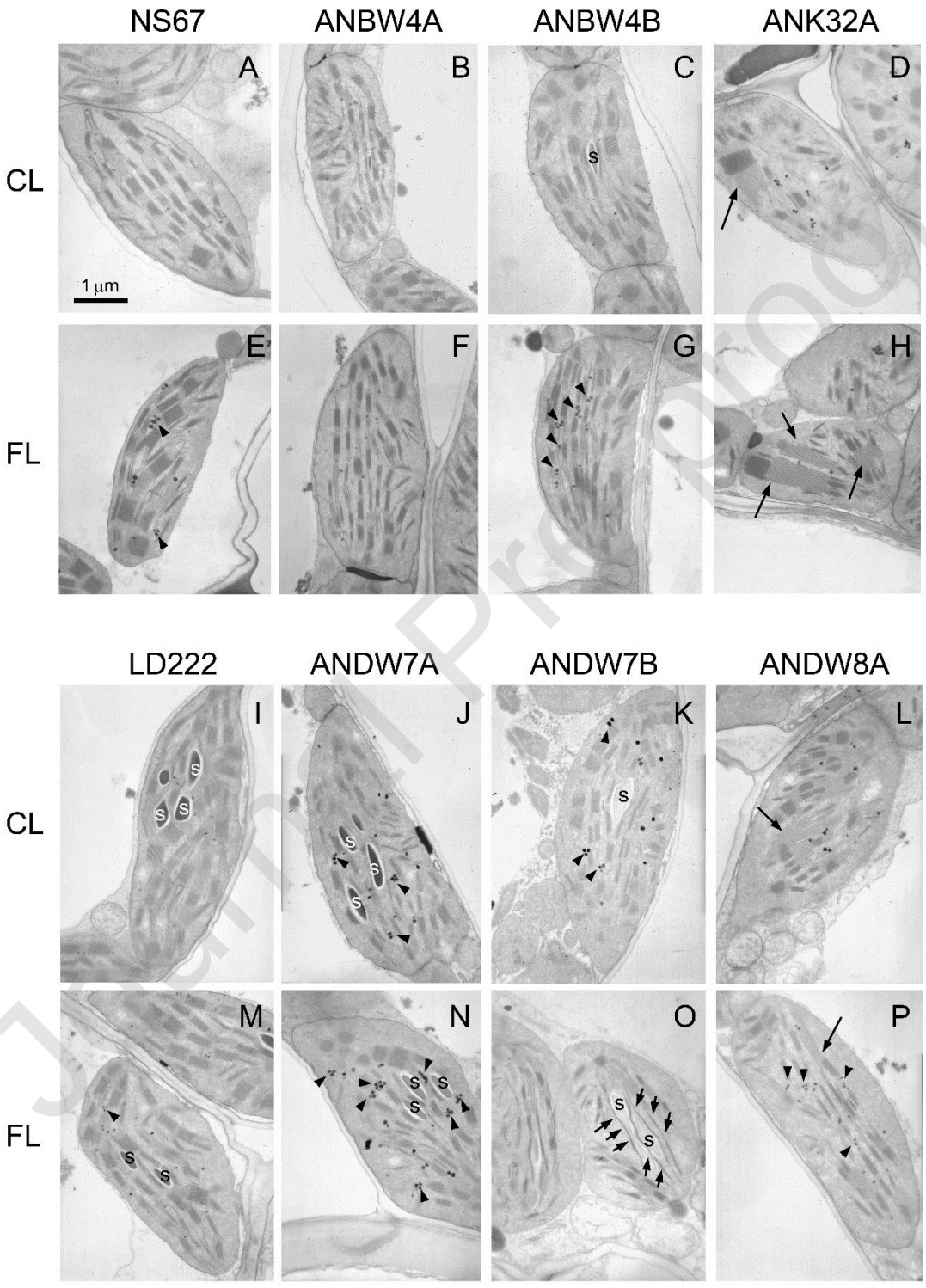

Fig. 7. Comparative transmission electron microscopy images of representative chloroplasts in WT *Triticum aestivum* (NS67, bread wheat) and *T. durum* (LD222, durum wheat) and in their respective *chlorina* mutants, cultivated in a continuous (CL) or fluctuating light regime (FL). Leaf samples were collected in the middle of photoperiod. s, starch granule.

(A, E) Chloroplasts with an extensive granal thylakoid system in NS67 cultured under CL or FLa.

(B, C) WT-like chloroplasts in ANBW4A and ANBW4B grown under CL.

(D) Chloroplast in ANK32A grown under CL with a reduced membrane system, including an array of single, parallel straight thylakoids (arrow) originating from a large granum.

(F) Chloroplast of ANBW4A grown under FL with smaller grana stacks than in NS67.

(G) Chloroplast of ANBW4B under FL with many plastoglobules clusters (arrowheads) interspersed in a thylakoid system with prevailing small grana.

(H) Two chloroplasts of ANK32A grown under FL, showing a reduced thylakoid system, but extensive arrays of parallel thylakoids.

(I, M) In LD222 cultured under CL or FL, chloroplasts with an extensive granal thylakoid system and a few primary starch granules (s).

(J, K) Thylakoid system with prevailing small grana stacks in chloroplasts of ANDW7A and ANDW7B grown under CL. Starch granules are present (s), as well as frequent plastoglobules (arrowheads).

(L) A chloroplast in ANDW8A under CL with a reduced thylakoid system and some arrays of single thylakoids (arrow).

(N) Chloroplast of ANDW7A grown in FL with a well-organized thylakoid system and very abundant in clusters of plastoglobules (arrowheads).

(O) Chloroplasts of ANDW7B grown in FL with thylakoid doublets (arrows) in a strongly reduced thylakoid system.

(P) A chloroplast of ANDW8A under FL with a reduced thylakoid system, very small grana, arrays of single thylakoids (arrow) and many plastoglobules (arrowheads).

3.5. Promotion of PSI excitation occurs in some *chlorina* mutants depending on light regime

Considering the concurrent alteration of ET and thylakoid organization in some *chlorina* mutants, we checked a possible alteration of excitation energy distribution between PSI and PSII. In WT and mutants, the energy distribution to PSII *dII* was a quite stable property over four weeks (Supplementary Fig. 9). In bread wheat, the main source of variation was ANK32A, in which the excitation of PSI prevailed over PSII (Fig. 8A). Although not revealed by significant Tukey's test, the promotion of PSI excitation occurred in ANDW7B durum wheat as well (Table 4). In other mutants (ANDW7A, ANDW8A, ANBW4B), energy distribution to PSI was promoted under CL, but not under FL (Fig. 8A; Table 3-4).

A lower *dII* could at least partly alleviate severely over-reduced states of the intersystem chain. *dII* and $\Delta Y(NO)$ were indeed inversely correlated and well fitted with a reciprocal function (*Adjusted* R^2=0.48, $P<10^{-5}$; Fig. 8B). Data distribution along the branch of the hyperbola indicated that low *dII* was associated with high $\Delta Y(NO)$, in fact ANK32A and ANDW7B laid indeed on the vertical asymptote. However, most points laid towards the horizontal asymptote. In particular, in ANDW7A and ANDW8A, a large delta in *dII* from CL to FL corresponded to negligible changes in $\Delta Y(NO)$.

[FIGURE 8 – 1 column fitting]

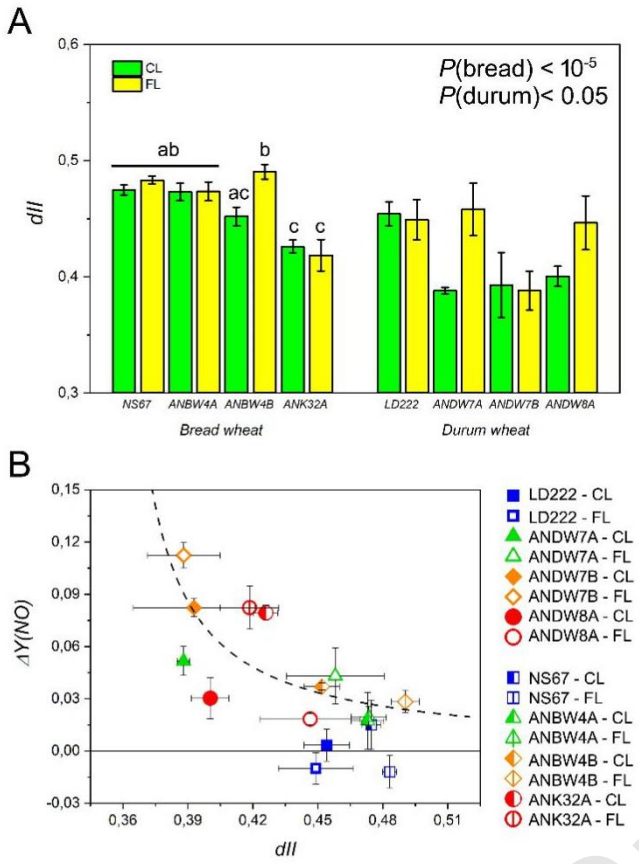

Fig. 8. Absorbed energy distribution to PSII (*dII*) in *chlorina* mutants of wheat grown under continuous (CL) or fluctuating (FL) light.

(A) *dII* values are means with SE of 4 measurements from independent plants sampled at four subsequent weeks. Data in histograms were analysed with one-way ANOVA separately for bread and durum wheat, resulting probability is reported in the graph. A post-hoc Tukey's test was run and results are reported in graphs (different letters mean statistically significant difference). In durum wheat, Tukey's test did not highlight the differences emerging from two-way ANOVA reported in Table 3.

(B) Covariation of *ΔY(NO)* and *dII*; the dashed line represents a hyperbolic regression.

3.6. Up-regulated alternative sinks in durum wheat mutants and ANBW4B help maintain the electron poise under a FL regime

An additional mechanism potentially involved in photoprotection is the exploitation of alternative electron sinks. Since they can have a specific role in the response to FL (Huang *et al.,* 2019), the downstream electron flow (J_A) driven to sinks alternative to carboxylation was quantified by parallel measurement of CO_2 assimilation and chlorophyll fluorescence. The high variability in J_A/J_{PSII} did not lead to significant one-way ANOVA (Supplementary Fig. 9, Fig. 9A). However, in durum wheat mutants, the dissection of mutant and light effects by two-way ANOVA indicated an emphasized J_A/J_{PSII} under FL (Fig. 9B). An up-regulated J_A is expected to remove electrons from the acceptor side of PSI, i.e. plants with strong alternative sinks should be able to keep $\Delta Y(NA)$ at a low level upon an increase in irradiance. The $\Delta Y(NA)$ *vs* J_A/J_{PSII} plot shown in Fig. 9C reveals some point clouds, in one of which all FL-grown durum *chlorina* mutants cluster together. As compared to the corresponding CL samples, their higher J_A/J_{PSII} was related to a capacity to retain $\Delta Y(NA)$ unvaried (ANDW8A) or to even decrease it (ANDW7A, ANDW7B). In bread wheat, the increment of J_A/J_{PSII} was limited to ANBW4B under FL, which clustered together with FL-grown durum wheat mutants (Fig. 9A-C). However, the time course of J_A/J_{PSII} and $\Delta Y(NA)$ showed their parallel decrease over time, indicating that the use of alternative sinks was progressively attenuated during the maturation of FL ANBW4B plants (Fig. 9D), in spite of being always higher than in the corresponding CL-grown plants (Fig. 9A).

[FIGURE 9 – 2 column fitting]

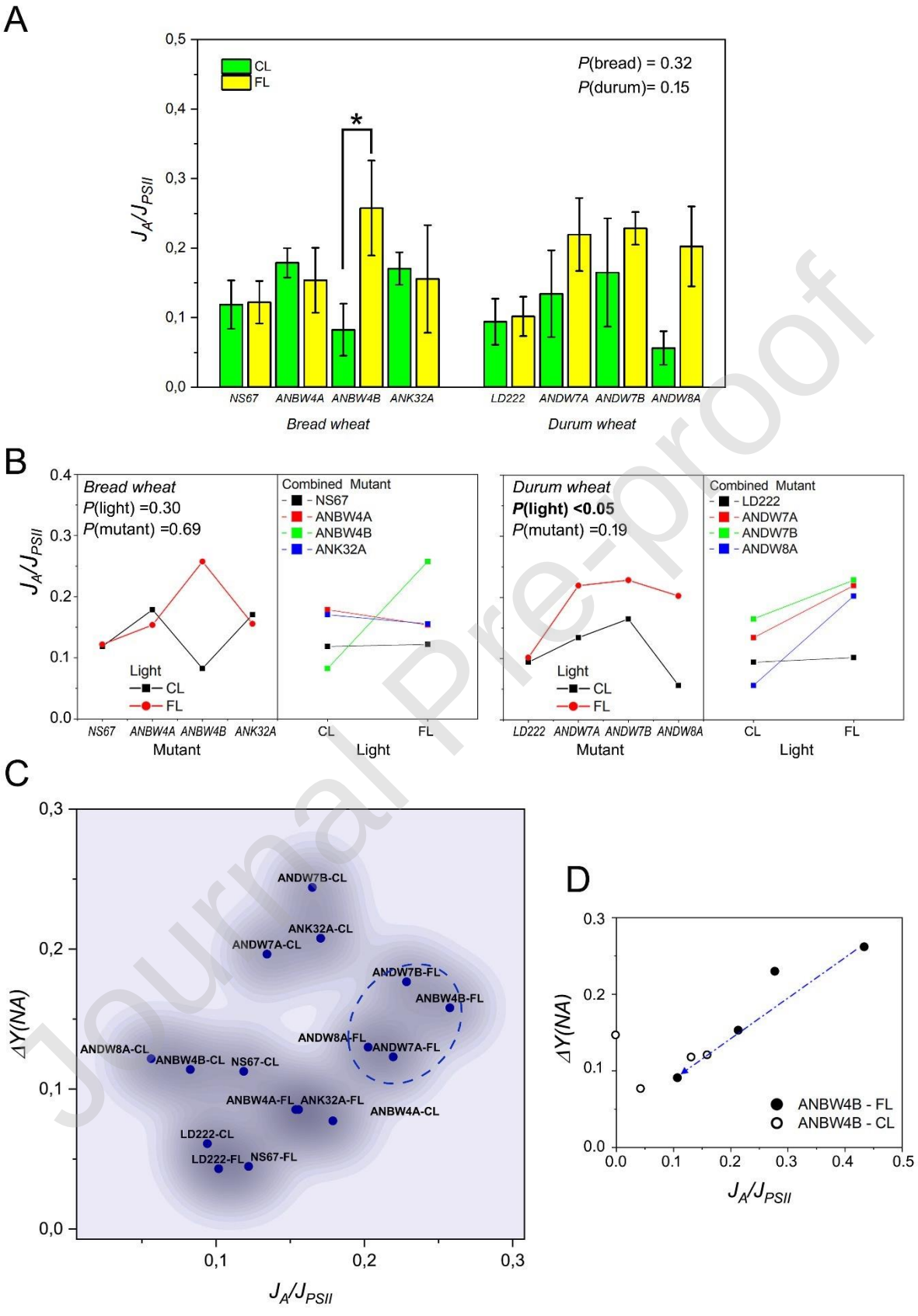

Fig. 9. Fraction of photosynthetic electron flow J_A/J_{PSII} driven to alternative electron sinks in chlorina mutants of wheat grown under continuous (CL) or fluctuating (FL) light.

(A) J_A/J_{PSII} values are means with SE of 4 measurements from independent plants sampled at four subsequent weeks. Data in histograms were analysed with one-way ANOVA separately for bread and durum wheat, resulting probability is reported in the graph. The asterisk marks a significant difference between ANBW4B grown either under CL or FL, according to a paired Student's *t* test.

(B) Combined means dissecting the effect of light and mutant with the corresponding probability obtained after two-way ANOVA.

(C) Covariation of $\Delta Y(NA)$ and J_A/J_{PSII} represented as a density map. The dashed circle includes all durum wheat mutants grown under FL plus ANBW4B under FL.

(D) Covariation of $\Delta Y(NA)$ and J_A/J_{PSII} over four weeks of monitoring of ANBW4B plants. Note that the data obtained from FL-grown plants are aligned and decreasing over time (dashed arrow).

3.7. Relationship between photosynthetic traits and final aboveground biomass

The 23 photosynthetic parameters measured in this work were analysed for their correlation to the final aboveground biomass accumulated by the plants (Fig. 2B, E). The observed trends were fitted using different models (linear, reciprocal, saturating, exponential decay) and the plasticity index (PI) was calculated according to Poorter *et al.* (2019). PI quantifies the relative distance between the extremes of each phenotypic parameter, and, in case of significant correlations, we considered parameters with PI $>|2.0|$ more informative for phenotyping (Poorter *et al.,* 2009). The fitted plots are shown in Supplementary Fig. 10 and the results are summarized in Table 5.

Many parameters showed a significant relationship with the final shoot biomass. The parameters best fitted with a saturation model, such as those linked to thermal dissipation [*NPQ*, *pmf*, *Y(PSI)/Y(PSII)*]

or CO_2 fixation, were basically invariable over a large range of resulting biomass. In fact, only a small subset of the other parameters varied in a sufficiently wide range between the extremes. Among them, a less effective control of the ET was very significantly related to lower shoot biomass. At the steady state, this emerged from *Y(NA)* and, upon a lightfleck, even more from *Y(NO)*, which exhibited the highest PI among all parameters. In spite of quite scattered points, interesting was also the negative correlation between J_A/J_{PSII} and the final shoot biomass. Considering our focus on the effect of growth in a FL regime, a comparative view of parameters under FL *vs* CL in the two most affected mutants ANDW7B and ANBW4B is also shown in Table 5. The parameters associated to a decrease in final aboveground biomass were more numerous and different in ANDW7B as compared to ANBW4B. Note that *ΔY(NA)*, which in ANBW4B resulted in a delta of 0.4, in ANDW7B was even excluded from fitting because ANDW7B under FL was an outlier point. Interestingly, a more prominent J_A/J_{PSII} was shared by both mutants.

	Parameter	Fit	R^2	Probability	PI	ANDW7B FL *vs* CL	ANBW4B FL *vs* CL
Steady-state activity of PSII	F_V/F_M	L	0.04	0.47	(-1.1)	-	-
	Y(II)	L	0.47	**<0.01**	-1.5	-	-
	Y(NO)	L	0.10	0.23	(-1.6)	0.2	-
	Y(NPQ)	L	0.26	0.05	(1.4)	0.2	-
	NPQ	S	0.57	**<0.01**	**2.1**	0.3	-
Steady-state activity of PSI	P_M/SPAD	L	0.15	0.14	(1.6)	-	-
	Y(I)	L	0.32	**<0.05**	1.3	-	-
	Y(NA)	R	0.82	**$<10^{-11}$**	**-4.0**	0.4	-
	Y(ND)	L	0.60	**$<10^{-3}$**	1.4	-	-
Steady-state carbon fixation capacity	A_{150}	S	0.72	**$<10^{-3}$**	1.9	-	-
	A_{500}	S	0.72	**$<10^{-3}$**	1.4	-	-
	A_{1150}	S	0.56	**<0.01**	1.4	-	-
	$Y(CO_2)$	S	0.67	**$<10^{-3}$**	**2.6**	0.2	-
	J_A/J_{PSII}	L	0.28	**<0.05**	**-4.6**	0.5	1.5
Comparative excitation and activity of PSI and PSII	*dII*	L	0.45	**<0.01**	1.3	-	-
	Y(I)/Y(II)	S	0.68	**$<10^{-3}$**	1.6	-	-
	pmf	S	0.40	**<0.05**	**2.5**	-	0.2
	g_{H^+}	R	0.54	**$<10^{-10}$**	**-2.2**	0.7	-

ΔpH generation and use	v_{H^+}	L	0	0.99	(2.0)	-	-
Dynamic regulation of electron pressure on photosystems	*ΔY(NO)*	E	0.68	**$<10^{-5}$**	**-9.4**	2.0	-
	ΔY(NA)	E	0.48	**$<10^{-6}$**	**-5.7**	nc	0.4
	Δ(1-qP)	L	0.53	**<0.01**	-1.1	-	-
	Y(qI)	L	0.44	**<0.01**	**-2.0**	-	0.2

Table 5 Summary of trait-dry weight relation curve analysis for all 16 combinations of genotypes and light regimes. Data plots are shown in Supplementary Fig. 10. Each plot of a photosynthetic trait (*y*) *vs* final aboveground dry weight (*x*) was fitted with the function indicated in column "Fit": linear (L; $y=ax+b$), saturating (S; $y=A_1-A_2e^{-bx}$), reciprocal [R; $y=a/(1+bx)$], exponential decay (E; $y=y_0+Ae^{-x/b}$). For each fit, the corresponding R^2 value is reported with the associated probability, in bold when significant. For all photosynthetic traits, the plasticity index (PI) was calculated as the ratio between the highest and lowest fitted value; positive PI means increasing trend, negative PI decreasing trends. PI values in parentheses correspond to traits yielding non-significant trends; bold numbers correspond to significant trends with a |PI|≥2.0. In the last two columns, for ANDW7B and ANBW4B, the delta FL vs CL between parameters normalized on CL-grown NS67 is reported when ≥0.2. nc, not calculated because ANDW7B under FL was excluded from the exponential fitting of *ΔY(NA)*.

4. DISCUSSION

The very variable severity of wheat *chlorina* mutants has been well-known for some time and interpreted as a direct consequence of the genetic lesion, leading not only to hindered antenna assembly (Falbel *et al.,* 1996), but also to a disturbance of the photosynthetic ET (Brestič *et al.,* 2015, 2016; Živčak *et al.,* 2019). In CL-grown plants, the steady state *Y(NA)* is the most straightforward index of such an alteration and confirms an already known severity series (NS67<ANBW4A≈ANBW4B<ANK32A for bread wheat and LD222<ANDW8A≈ANDW7A<ANDW7B for durum wheat; Živčak *et al.*, 2019). The buffering effect of polyploidy explains why hexaploid ANBW4B performs much better than tetraploid ANDW7B under CL (Dubcovsky and Dvorak, 2007; Živčak *et al.,* 2019). Absence of other strong steady-state

deregulations indicates that, in the CL sector of SPPU, the plants already expressed a quite mature phenotype during the four weeks of analyses, confirming a known tendency of *chlorina* wheat to recover to WT phenotype (Fig. 2; Brestič *et al.,* 2016). Therefore, under a stable photon flux, the mutants are capable of stabilising their light energy management, minimising the disturbance of the ET and preserving their capacity of ATP synthesis (ν_{H+}) and steady-state carbon fixation (A_{500}) (Fig. 3A-B, 5D). However, unexpectedly, here we document that in most wheat *chlorina* mutants an effective light energy management can still be possible even under a fluctuating light regime.

4.1. Lightflecks challenge the regulation of the photosynthetic electron poise in *chlorina* mutants

The defect in Chl synthesis of *chlorina* wheat is deemed adverse to a proper chloroplast redox homeostasis especially when irradiance suddenly increases (Brestič *et al.,* 2015, 2016; Wang *et al.,* 2018; Živčak *et al*., 2019). Upon a fast rise in irradiance, an excess of electrons enters the intersystem ET chain, increasing the probability that the photosystems are inactivated (Yamori, 2016; Armbruster *et al.,* 2017). A *reducing burst* causes indeed an over-reduction of PSI during the first 20 s of the rise, when the *pmf* seems predominantly formed by its electric field component $\Delta\psi$ (Huang *et al.,* 2019), which is a causal factor for PSII photodamage as well (Davis *et al.,* 2016). However, in less than one minute the generation of the trans-thylakoidal ΔpH re-establishes the equilibrium between $\Delta\psi$ and ΔpH in *pmf* (Huang *et al.,* 2019). *NPQ* induction by ΔpH down-regulates the electron flow-in from PSII into the chain and favours the oxidized state of PSI, which is a necessary condition to preserve the photosynthetic membrane (Trissl, 1997; Shimakawa and Miyake, 2018a; Kadota *et al.,* 2019). Different from both WT, all *chlorina* mutants grown under CL, except ANBW4A, are compromised to some extent in the control of the reducing burst and tend to accumulate reduced plastoquinone during a lightfleck (Fig. 6A-C). In a well-regulated system, the control of PSI oxidation depends primarily on the activation of CEF (Shimakawa and Miyake, 2018b) and, accordingly, the degree of deregulation of ET in *chlorina* wheat was just roughly specular to the reduction in their capacity of operating CEF (see *Y(PSI)/Y(PSII)* and also Živčak *et al.,*

2019). In durum wheat mutants, some discrepancies between *Y(PSI)/Y(PSII)* and *pmf* can be suggestive of an altered composition of *pmf*, which can potentially make their photosystems more prone to photodamage than in bread wheat (Armbruster *et al.,* 2017). Upon the single lightfleck simulated with Dual-PAM, this inference is specifically supported by increased *Y(qI)* in the weakest mutant, ANDW7B (Fig. 6E).

4.2. The mutated locus *cn-B1b* negatively affects the development of a FL phenotype

In the long term, plants growing in the FL sector of SPPU were expected to develop a *FL phenotype*, a condition mainly studied in the model dicot *Arabidopsis thaliana* and comprising adjustments in leaf morphology, stomatal responses, light use and carbon fixation efficiency (Vialet-Chabrand *et al.,* 2017; Kaiser *et al.,* 2018b; Matthews *et al.,* 2018; Schneider *et al.,* 2019). Growth under FL increases a plant's ability to use the light energy for carbon fixation (Vialet-Chabrand *et al.,* 2017), probably exploiting a superior dynamic regulation of the thylakoid membrane upon sudden rises and drops in irradiance (Schumann *et al.,* 2017). The improvement of the overall efficiency of ET regulation is related to a global reprogramming of photosynthetic gene expression, leading to a decrease in *Y(PSII)* and, conversely, an up-regulation of proteins related to CEF and *NPQ* (Schneider *et al.,* 2019; Niedermaier *et al*., 2020). However, in our experiment, NS67 and LD222 changed negligibly between CL and FL sectors with respect to all steady-state parameters, supporting the concept that wheat cultivars can acclimate promptly and effectively to sunflecks (Salter *et al*., 2019). Low $\Delta Y(NO)$ and $\Delta Y(NA)$ in both WT cultivars reveal indeed an intrinsic efficiency in ET regulation already when plants are grown under CL. In the FL regime, furtherly lower $\Delta Y(NO)$ and $\Delta Y(NA)$ reflect successful adjustments of the redox homeostasis, testifying to the occurrence of a FL-specific reprogramming (Fig. 6A-C). In their chloroplasts, the abundance of thylakoid-associated plastoglobules is also evidence for the development of a FL phenotype. By analogy, in *A. thaliana* an up-regulated plastoglobule proteome under FL is the structural result of a more

dynamic metabolism of thylakoidal pigments and prenyl-lipids (Schneider *et al.,* 2019; Niedermaier *et al*., 2020).

We anticipated that the stronger the deregulation of ET in a *chlorina* mutant, the worse its performance under the unceasing challenge of lightflecks in FL. However, strikingly this was not the case and, in terms of shoot biomass, only the plants carrying the mutated locus *cn-B1b* (ANBW4B and ANDW7B) were strongly inhibited (Fig. 2). ANBW4B carries the same mutation in subgenome B as ANDW7B, but with a lower severity, which can be due to a partial compensation of the recessive *cn* mutation by additional subgenome D (International Wheat Genome Sequencing Consortium, 2018). Therefore, especially ANDW7B is exemplary for a failure to develop an effective FL-phenotype (Fig. 6C). Its defects in light energy management are indeed aggravated under FL, when the miscontrol of ET is exacerbated by a lower capacity to generate *NPQ*, because of less CEF and also a tendency to increase the ATP synthase activity (Fig. 4D, 5A-C). Absence of any obvious order in thylakoid architecture well reflects ANDW7B instability under FL. Unique among our *chlorina* mutants, its long thylakoid doublets were previously shown in CD3 *chlorina* wheat (Allen *et al.,* 1988) and are very similar to the long thylakoid appressions assembled in mutants of *A. thaliana* lacking thylakoid curvature factors (CURT) (Armbruster *et al.,* 2013; Fig. 7O). Long thylakoid doublets are structurally unfavourable to the flexible lateral heterogeneity of photosystems, thus preventing a proper co-regulation of linear and cyclic ETs. In particular, ANDW7B under FL and CURT mutants share a decrease in CET and *NPQ* (Fig. 4D, 5A). Among the expected consequences, a chronic over-reduction of plastoquinone occurs in ANDW7B grown under FL (Fig. 4C). In addition, achieving the lowest A_{150} among all samples, ANDW7B will lose opportunities for carbon fixation during the light drops after each lightfleck. Altogether, these results well explain the very low biomass accumulation in ANDW7B under FL. Also the bread wheat counterpart ANBW4B has a reduced final biomass under FL, but it tends more definitely to re-establish a WT phenotype. Nonetheless, chloroplast integrity is preserved at the cost of a large metabolic investment, shown by the

very abundant plastoglobules (Fig. 7G; Schneider *et al.,* 2019) and also by the occurrence of compensatory mechanisms, as discussed in the following section.

4.3. Compensatory responses can allow FL acclimation in *chlorina* mutants

A comparison between ANDW7B and the other two durum wheat mutants ANDW7A and ANDW8A suggests that the impact of lightflecks can be alleviated by compensatory responses, such as modulations of energy distribution between PSI and PSII (Fig. 8A). The problem of excitation energy balancing is interesting in *chlorina* wheat, because PSI/PSII stoichiometry may change in favour of PSII and be one possible reason for reduced CEF (Brestič *et al.,* 2015; Nicol *et al.,* 2019; Živčak *et al.,* 2019). In all durum wheat mutants under CL, excitation shift towards PSI can just be an attempt to promote CEF. The underlying mechanisms, which require fine adjustments of the antenna sharing between PSI and PSII (Goldschmidt-Clermont and Bassi, 2015), remain unknown in the context of reduced antenna complement in *chlorina* wheat. However, the *chlorina* mutants do maintain an unexpected degree of flexibility in the excitation distribution between the two photosystems (Fig. 8). In ANDW7A and ANDW8A, in fact, under FL a re-equilibration of excitation towards PSII occurs. Addressing the biological meaning of the high-light-induced PSII antenna dephosphorylation, Mekala *et al.* (2015) proposed that, while high irradiance provides both photosystems with an excess of excitation, an antenna organization potentially favouring PSII can promptly promote the linear ET upon a sudden shading. Accordingly, given the low $Y(CO_2)$ of *chlorina* durum wheat (Fig. 2C), in a FL regime a constitutive preferential excitation of PSII may help the electron flow-in from PSII to final acceptors during shadeflecks, thus limiting energy losses after each light rise. The worst performer ANDW7B does not take advantage of such an acclimative mechanism and maintains instead a preferential excitation of PSI, which may contribute to further decrease its biomass yield (Fig. 8A).

That the promotion of PSII excitation under FL does not result in any increase in *Y(NO)* or *Y(NA)* in ANDW7A and ANDW8A appears counterintuitive; yet this can be possible through the parallel exploitation of electron sinks alternative to photosynthesis and photorespiration (Fig. 9A). Among the acceptor-side mechanisms to keep PSI oxidised (Shimakawa and Miyake, 2018a), alternative electron sinks can have a special relevance in stressed plants, as demonstrated in various angiosperms, including drought-treated wheat (Makino *et al.,* 2002; Hirotsu *et al.,* 2004; Živčak *et al.,* 2013; Cai *et al.,* 2017). A major alternative sink in angiosperms is the water-water cycle (WWC), responsible for a pseudocyclic ET through an apparently futile use of electrons for O_2 photo-reduction (Makino *et al.,* 2002). When the ΔpH is still low during the first seconds of a lightfleck, WWC can allow the fast oxidation of PSI, strongly indicating a key regulatory role of WWC in FL regimes (Huang *et al.,* 2019). Durum wheat mutants show indeed a tendency to increase their capacity to drive electrons to alternative sinks under FL, helping electron removal from PSI (Fig. 9A-C). In fact, the largest gain in J_A/J_{PSII} is found in ANDW8A, which, however and different to ANDW7A, surprisingly exhibits an altered thylakoid organization (Fig. 7P). The chloroplast structures we have shown represent final stages in the mutant development and strongly suggest that an acclimatized growth under FL can be achieved in alternative thylakoid architectures. In this respect, the response of ANK32A to FL is particularly instructive.

In ANK32A, the (poor) control of ET does not further worsen under FL and $\Delta Y(NA)$ even improves (Fig. 6C), in spite of no compensation by alternative electron flow (Fig. 9A). The most evident feature of ANK32A chloroplasts is the assembly of large grana stacks connected to regular long arrays of single thylakoids (Fig. 7H). Such a thylakoid arrangement, already known in other *chlorina* wheats (Falbel *et al.,* 1996), appears paradoxically permissive to a successful acclimation to FL, and its prevalence under FL challenges the idea that thylakoid anomalies in *chlorina* wheat would be the mere reflection of a lower abundance of antennae (Falbel *et al.,* 1996). In fact, a loss of antennae caused by depletion of Chl and/or LHCB proteins can lead to smaller or fewer grana (Kim *et al.,* 2009; Friedland *et al.,* 2019), or even have

no effect on thylakoid stacking (Nicol *et al.,* 2019). Differently, *chlorina* wheats explore a variety of alternatives, including spatially misordered individual stacks (Wang *et al.,* 2018) and anomalous relations between stacked and unstacked regions (Falbel *et al.,* 1996). For an effective response to FL, current models of PSI-PSII interaction require the membrane complexes to be mixable at the grana margins and, consequently, the thylakoid stacking to be modulatable as well (Grieco *et al.,* 2015; Yokono and Akimoto, 2018; Rantala *et al*., 2020). However, some static thylakoid configurations can still allow for a sufficient ET control (Giovanardi *et al.,* 2018) and, in spite of its defects, ANK32A could be an extreme example. The very regular thylakoid arrays connected to large grana in ANK32A could be not just the consequence of a reduced LHCII content (Allen *et al.,* 1988; Falbel *et al.,* 1996), but provide an additional compensatory structural frame against defective ET. Similarly, ANDW8A, which successfully acclimates to a FL regime without any loss of biomass as compared to CL, can profitably count not only on adjustable alternative electron flow and excitation distribution between photosystems (Fig. 8A, 9A), but also on some thylakoid arrays connected to grana (Fig. 7P).

5. Conclusions: can photosynthesis-related parameters be used in a predictive perspective?

In *chlorina* wheat mutants, different compensatory mechanisms can be exploited with varying importance depending on the mutated locus and the genomic context, and finally result in FL-acclimated phenotypes. Nevertheless, in contrast to a repeatedly proposed concept (Jin *et al.,* 2016; Song *et al.,* 2017; Wang *et al.,* 2018), in our study a reduced Chl content did not lead to more productive wheat plants. An overall view suggests that the reduced performance of mutants can be a direct effect of ET disturbance and an indirect consequence of a larger fraction of metabolic energy that is deviated to compensatory mechanisms to ensure the chloroplast redox homeostasis.

An ultimate goal of photosynthetic plant phenotyping is to use easily measurable parameters in order to screen and select advantageous traits in crops, including the challenge of enhancing plant

performance under a FL regime (van Bezouw *et al.,* 2019). Among the 23 photosynthetic parameters evaluated in this work, only few of them combined two desirable characteristics for a profitable use in plant selection under FL regime: very significant correlation to biomass accumulation and wide PI. Some of them are very informative of plant physiology, but inadequate to automated phenotyping, because they require time-consuming gas exchange measurements [J_A/J_{PSII}, $Y(CO_2)$] or leaf absorption measurements [$Y(NA)$]. Since whole plant photosynthetic phenotyping exploits fast-detectable light emission or reflection, we propose that lightfleck-probed $Y(NO)$ can have a great potential for the automated screening of Chl-depleted wheat mutants with respect to their potential productivity.

CRediT Authors statement

Lorenzo Ferroni: conceptualization, investigation, formal analysis, writing – original draft, writing – review and editing, supervision
Marek Živčak: conceptualization, formal analysis, data curation, writing – review and editing
Oksana Sytar: investigation, formal analysis, writing – original draft
Marek Kovár: software, investigation, formal analysis, data curation
Nobuyoshi Watanabe: resources
Simonetta Pancaldi: investigation, formal analysis
Costanza Baldisserotto: investigation, formal analysis
Marián Brestič: conceptualization, writing – review and editing, supervision, funding acquisition

CONFLICT OF INTEREST

The authors declare no conflict of interest.

AUTHOR CONTRIBUTIONS

LF, MZ, MB conceived the experiment; NW contributed the wheat mutants collection; MK set up and managed the SPPU facility for the experiment; LF, OS, MZ, MK performed the experiment and collected data; LF, OS, MZ, MK, CB, SP, MB analysed the data; LF, OS drafted the manuscript; LF, MB supervised the research; all authors reviewed and edited the manuscript.

DATA AVAILABILITY

Raw data are available upon request from the authors.

Declaration of interests

The authors declare that they have no known competing financial interests or personal relationships that could have appeared to influence the work reported in this paper.

ACKNOWLEDGMENTS

This study was performed within the European Plant phenotyping Network 2020 (EPPN^{2020}) and the Slovak Plant Phenotyping Network (SKPPN). The Authors are grateful for the financial support provided by the Access to Research Infrastructures activity in the Horizon2020 Programme of the EU (EPPN^{2020} Grant Agreement 731013) for the experiment "TriPUDIUM- TRIticum Photosynthesis Under Drought and fluctuating Irradiance: Use of Mutants phenotyping to approach crop photosynthetic regulation". Lenka Botyanszka, Klaudia Brücková, Erik Chovanček (Slovak University of Agriculture in Nitra) and Paola Boldrini (Electron Microscopy Centre of the University of Ferrara) are gratefully thanked for their excellent technical support. Prof. Katarina Olšovská (Slovak University of Agriculture in Nitra) is kindly thanked for her support to accurate administration of the project.

LEGENDS FOR SUPPLEMENTARY INFORMATION

Supplementary Figure 1. Environmental parameters monitoring at the Slovak PlantScreen^{TM} Phenotyping Unit.

Supplementary Figure 2. Light intensity variation during Dual-PAM measuring routine for analysis of PSII and PSI parameters.

Supplementary Figure 3. CO_2 fixation properties as emerging from gas exchange analyses.

Supplementary Figure 4. Time course of parameters related to PSII activity as emerging from Dual-PAM analyses.

Supplementary Figure 5. Time course of parameters related to PSI activity as emerging from Dual-PAM analyses.

Supplementary Figure 6. Time course of parameters related to the generation and use of the trans-thylakoidal proton motive force.

Supplementary Figure 7. Time course of parameters related to the dynamic regulation of photosynthesis.

Supplementary Figure 8. Examples of thylakoid architectures in chloroplasts of *chlorina* mutants of wheat.

Supplementary Figure 9. Time course of the energy distribution to PSII (*dII*) and the ET to electron sinks alternative to photosynthesis (J_A/J_{PSII}).

Supplementary Figure 10. Plots of measured photosynthesis-related parameters *vs* final aboveground biomass accumulated by *Triticum* plants.

REFERENCES

Albanese, P., Melero, R., Engel, B.D., Grinzato, A., Berto, P., Manfredi, M., Chiodoni, A., Vargas, J., Sorzano, C.Ó.S., Marengo, E., Saracco, G., Zanotti, G., Carazo, J.M., Pagliano, C., 2017. Pea PSII-LHCII supercomplexes form pairs by making connections across the stromal gap. Sci. Rep. 7(1), 10067. https://doi: 10.1038/s41598-017-10700-8.

Allen, K.D., Duysen, M.E., Staehelin, L.A., 1988. Biogenesis of thylakoid membranes is controlled by light intensity in the conditional chlorophyll *b*-deficient CD3 mutant of wheat. J. Cell Biol. 107(3), 907-919. https://doi: 10.1083/jcb.107.3.907

Anderson, J. M., 2012. Lateral heterogeneity of plant thylakoid protein complexes: early reminiscences. Phil. Trans. R. Soc. B 367(1608), 3384–3388. https://doi:10.1098/rstb.2012.0060

Armbruster, U., Labs, M., Pribil, M., Viola, S., Xu, W., Scharfenberg, M., Hertle, A.P., Rojahn, U., Jensen, P.E., Rappaport, F., Joliot, P., Dörmann, P., Wanner, G., Leister, D., 2013. Arabidopsis CURVATURE THYLAKOID1 proteins modify thylakoid architecture by inducing membrane curvature. Plant Cell 25, 2661–2678. https://doi: 10.1105/tpc.113.113118

Armbruster, U., Correa Galvis, V., Kunz, H.-H., Strand, D.D., 2017. The regulation of the chloroplast proton motive force plays a key role for photosynthesis in fluctuating light. Curr. Opin. Plant Biol. 37, 56–62. https://doi: 10.1016/j.pbi.2017.03.012

Bailleul, B., Cardol, P., Breyton, C., Finazzi, G., 2010. Electrochromism: a useful probe to study algal photosynthesis. Photosynth. Res. 106(1-2), 179-89. https://doi: 10.1007/s11120-010-9579-z.

Bernacchi, C.J., Portis, A.R., Nakano, H., von Caemmerer, S., Long, S.P., 2002. Temperature response of mesophyll conductance. Implications for the determination of Rubisco enzyme kinetics and for limitations to photosynthesis in vivo. Plant Physiol. 130, 1992–1998. https://doi: 10.1104/pp.008250

Björkman, O., Demmig-Adams, B., 1995. Regulation of photosynthetic light energy capture, conversion, and dissipation in leaves of higher plants. In: Schulze ED, Caldwell MM (eds) Ecophysiology of photosynthesis. Springer, Berlin, pp 17–47.

Brestič, M., Živčak, M., Kunderlikova, K., Sytar, O., Shao, H., Kalaji, H.M., Allakhverdiev, S.I., 2015. Low PSI content limits the photoprotection of PSI and PSII in early growth stages of chlorophyll *b*-deficient wheat mutant lines. Photosynth. Res. 125(1-2), 151-166. https://doi: 10.1007/s11120-015-0093-1.

Brestič, M., Živčak, M., Kunderlikova, K., Allakhverdiev, S.I., 2016. High temperature specifically affects the photoprotective responses of chlorophyll *b*-deficient wheat mutant lines. Photosynth. Res. 130(1-3), 251-266. https://doi: 10.1007/s11120-016-0249-7

Cai, Y.F., Yang, Q.Y., Li, S.F., Wang, J.H., Huang, W., 2017. The water-water cycle is a major electron sink in *Camellia* species when CO_2 assimilation is restricted. J. Photochem. Photobiol. B Biol. 168, 59–66. https://doi:10.1016/j.jphotobiol.2017.01.024

Davis, G.A., Kanazawa, A., Schöttler, M.A., Kohzuma, K., Froehlich, J.E., Rutherford, A.W., Satoh-Cruz, M., Minhas, D., Tietz, S., Dhingra, A., Kramer, D.M., 2016. Limitations to photosynthesis by proton motive force-induced photosystem II photodamage. eLife 5, e16921. https://doi:10.7554/eLife.16921.

Dubcovsky, J., Dvorak, J., 2007. Genome plasticity a key factor in the success of polyploid wheat under domestication. Science 316, 1862–1866.

Edwards, C.E., Ewers, B.E., McClung, C.R., Lou, P., Weinig, C., 2012. Quantitative variation in water-use efficiency across water regimes and its relationship with circadian, vegetative, reproductive, and leaf gas-exchange traits. Mol. Plant. 5(3), 653-668. https://doi: 10.1093/mp/sss004.

Falbel, T.G., Meehl, J.B., Staehelin, L.A., 1996. Severity of mutant phenotype in a series of chlorophyll-deficient wheat mutants depends on light intensity and the severity of the block in chlorophyll synthesis. Plant Physiol. 112(2), 821-832. https://doi: 10.1104/pp.112.2.821

Ferroni, L., Suorsa, M., Aro, E.-M., Baldisserotto, C., Pancaldi, S., 2016. Light acclimation in the lycophyte *Selaginella martensii* depends on changes in the amount of photosystems and on the flexibility of the light-harvesting complex II antenna association with both photosystems. New Phytol. 211(2), 554-568. https://doi: 10.1111/nph.13939.

Ferroni, L., Cucuzza, S., Angeleri, M., Aro, E.-M., Pagliano, C., Giovanardi, M., Baldisserotto, C., Pancaldi, S., 2018. In the lycophyte *Selaginella martensii* is the "extra-qT" related to energy spillover? Insights into photoprotection in ancestral vascular plants. Env. Exp. Bot. 154, 110–122. https://doi: 10.1016/j.envexpbot.2017.10.023.

Friedland, N., Negi, S., Vinogradova-Shah, T., Wu, G., Ma, L., Flynn, S., Kummssa, T., Lee, C.-H., Sayre, R.T., 2019. Fine-tuning the photosynthetic light harvesting apparatus for improved photosynthetic efficiency and biomass yield. Sci. Rep. 9, 13028. https://doi.org/10.1038/s41598-019-49545-8

Genty, B., Briantais, J.-M., Baker, N.R., 1989. The relationship between the quantum yield of photosynthetic electron transport and quenching of chlorophyll fluorescence. Biochim. Biophys. Acta - General Subjects 990 (1), 87-92. https://doi.org/10.1016/S0304-4165(89)80016-9

Giovanardi, M., Pantaleoni, L., Ferroni, L., Pagliano, C., Albanese, P., Baldisserotto, C., Pancaldi, S., 2018. In pea stipules a functional photosynthetic electron flow occurs despite a reduced dynamicity of LHCII association with photosystems. Biochim. Biophys. Acta – Bioenerg. 1859, 1025-1038. https://doi.org/10.1016/j.bbabio.2018.05.013

Goldschmidt-Clermont, M., Bassi, R., 2015. Sharing light between two photosystems: mechanism of state transitions. Curr. Opin. Plant Biol. 25, 71–78. https://doi.org/10.1016/j.pbi.2015.04.009

Grieco, M., Tikkanen, M., Paakkarinen, V., Kangasjärvi, S., Aro, E.-M., 2012. Steady-state phosphorylation of light-harvesting complex II proteins preserves photosystem I under fluctuating white light. Plant Physiol. 160(4), 1896-910. https://doi.org/10.1104/pp.112.206466.

Grieco, M., Suorsa, M., Jajoo, A., Tikkanen, M., Aro, E.-M., 2015. Light-harvesting II antenna trimers connect energetically the entire photosynthetic machinery - including both photosystems II and I. Biochim. Biophys. Acta 1847(6-7), 607-19. https://doi.org/ 10.1016/j.bbabio.2015.03.004.

Harley, P.C., Loreto, F., Di Marco, G., Sharkey, T.D., 1992. Theoretical considerations when estimating the mesophyll conductance to CO_2 flux by analysis of the response of photosynthesis to CO_2. Plant Physiol. 98, 1429–1436. https://doi.org/10.1104/pp.98.4.1429

Hendrickson, L., Furbank, R.T., Chow, W.S., 2004. A simple alternative approach to assessing the fate of absorbed light energy using chlorophyll fluorescence. Photosynth. Res. 82, 73–81. https://doi.org/10.1023/B:PRES.0000040446.87305.f4

Hirotsu, N., Makino, A., Ushio, A., Mae, T., 2004. Changes in the thermal dissipation and the electron flow in the water-water cycle in rice grown under conditions of physiologically low temperature. Plant Cell Physiol. 45, 635–644. https://doi.org/10.1093/pcp/pch075

Huang, W., Suorsa, M., Zhang, S.B., 2018. In vivo regulation of thylakoid proton motive force in immature leaves. Photosynth. Res. 138(2), 207-218. https://doi.org/ 10.1007/s11120-018-0565-1.

Huang, W., Yang, Y.J., Zhang, S.B., 2019. Photoinhibition of photosystem I under fluctuating light is linked to the insufficient ΔpH upon a sudden transition from low to high light. Env. Exp. Bot.160, 112–119. https://doi.org/ 10.1016/j.envexpbot.2019.01.012.

Huang, W., Yang, S.J., Zhang, S.B., Zhang, J.L., Cao, K.F., 2012. Cyclic electron flow plays an important role in photoprotection for the resurrection plant *Paraboea rufescens* under drought stress. Planta 235, 819-828. https://doi.org/ 10.1007/s00425-011-1544-3.

Jiang, H., Wang, N., Jian, J., Wang, C., Xie, Y., 2019. Rapid mapping of a chlorina mutant gene *cn-a1* in hexaploid wheat by bulked segregant analysis and SNP genotyping arrays. Crop & Pasture Sci. 70(10), 827-836. https://doi.org/10.1071/CP19165

Jin, H., Li, M., Duan, S., Fu, M., Dong, X., Liu, B., Feng, D., Wang, J., Wuang, H.B., 2016. Optimization of light-harvesting pigment improves photosynthetic efficiency. Plant Physiol. 172, 1720–1731. https://doi.org/ 10.1104/pp.16.00698.

International Wheat Genome Sequencing Consortium, 2018. Shifting the limits in wheat research and breeding using a fully annotated reference genome. Science 361, 661.

Kaiser, E., Morales, A., Harbinson, J., 2018a. Fluctuating light takes crop photosynthesis on a rollercoaster ride. Plant Physiol. 176, 977-989. https://doi.org/10.1104/pp.17.01250.

Kaiser, E., Matsubara, S., Harbinson, J., Heuvelink, E., Marcelis, L.F.M., 2018b. Acclimation of photosynthesis to lightflecks in tomato leaves: interaction with progressive shading in a growing canopy. Physiol. Plant. 162, 506-517. https://doi.org/10.1111/ppl.12668.

Kalaji, H.M., Schansker, G., Ladle, R.J., Goltsev, V., Bosa, K., Allakhverdiev, S.I., Brestič, M., Bussotti, F., Calatayud, A., Dąbrowski, P., Elsheery, N.I., Ferroni, L., Guidi, L., Hogewoning, S.W., Jajoo, A., Misra, A.N., Nebauer, S.G., Pancaldi, S., Penella, C., Poli, D., Pollastrini, M., Romanowska-Duda, Z.B., Rutkowska, B., Serôdio, J., Suresh, K., Szulc, W., Tambussi, E., Yanniccari, M., Živčak, M., 2014. Frequently asked questions about in vivo chlorophyll fluorescence: practical issues. Photosynth. Res. 122(2), 121-158. https://doi.org/ 10.1007/s11120-014-0024-6.

Kalaji, H.M., Schansker, G., Brestič, M., Bussotti, F., Calatayud, A., Ferroni, L., Goltsev, V., Guidi, L., Jajoo, A., Li, P., Losciale, P., Mishra, V.K., Misra, A.N., Nebauer, S.G., Pancaldi, S., Penella, C., Pollastrini, M., Suresh, K., Tambussi, E., Yanniccari, M., Živčak, M., Cetner, M.D., Samborska, I.A., Stirbet, A., Olsovska, K., Kunderlikova, K., Shelonzek, H., Rusinowski, S., Bąba, W., 2017. Frequently asked questions about chlorophyll fluorescence, the sequel. Photosynth. Res. 132(1), 13-66. https://doi.org/ 10.1007/s11120-016-0318-y

Kadota, K., Furutani, R., Makino, A., Suzuki, Y., Wada, S., Miyake, C., 2019. Oxidation of P700 induces alternative electron flow in photosystem I in wheat leaves. Plants 8, 152. https://doi.org/10.3390/plants8060152

Kim, E.-H., Li, X.-P., Razeghifard, R., Anderson, J.M., Niyogi, K.K., Pogson, B.J., Chow, W.S., 2009. The multiple roles of light-harvesting chlorophyll a/b-protein complexes define structure and optimize function of *Arabidopsis* chloroplasts: A study using two chlorophyll *b*-less mutants. Biochim. Biophys. Acta 1787, 973–984. https://doi.org/10.1016/j.bbabio.2009.04.009

Klughammer, C., Schreiber, U., 1994. An improved method, using saturating light pulses, for the determination of photosystem I quantum yield via $P700^+$-absorbance changes at 830 nm. Planta 192, 261-268. https://doi.org/10.1007/BF01089043

Kosuge, K., Watanabe, N., Kuboyama, T., 2011. Comparative genetic mapping of the chlorina mutant genes in genus *Triticum*. Euphytica 179, 257–263. https://doi.org/10.1007/s10681-010-0302-0

Koval, S.F., 1997. The catalogue of near-isogenic lines of Novosibirskaya 67 common wheat and principles of their use in experiments. Russ. J. Genet. 33, 995–1000.

Krall, J.P., Edwards, G.E., 1992. Relationship between photosystem II activity and CO_2 fixation in leaves. Physiol. Plant. 86 (1), 180-187.

Makino, A., Miyake, C., Yokota, A., 2002. Physiological functions of the water–water cycle (Mehler reaction) and the cyclic electron flow around PSI in rice leaves. Plant Cell Physiol. 43, 1017–1026. https://doi.org/10.1093/pcp/pcf124

Matthews, J.S.A., Vialet-Chabrand, S., Lawson, T., 2018. Acclimation to fluctuating light impacts the rapidity of response and diurnal rhythm of stomatal conductance. Plant Physiol. 176, 1939–1951. https://doi.org/10.1104/pp.17.01809

Mekala, N.R., Suorsa, M., Rantala, M., Aro, E.-M., Tikkanen, M., 2015. Plants actively avoid state transitions upon changes in light intensity: role of light-harvesting complex II protein dephosphorylation in high light. Plant Physiol. 168, 721–738. https://doi.org/10.1104/pp.15.00488

Munekage, Y., Hojo, M., Meurer, J., Endo, T., Tasaka, M., Shikanai, T., 2002. PGR5 is involved in cyclic electron flow around photosystem I and is essential for photoprotection in *Arabidopsis*. Cell 110, 361–371. https://doi.org/10.1016/s0092-8674(02)00867-x

Nicol, L., Nawrocki, W.J., Croce, R., 2019. Disentangling the sites of non-photochemical quenching in vascular plants. Nature Plants 5, 1177–1183. https://doi.org/1 0.1038/s41477-019-0526-5.

Niedermaier, S., Schneider, T., Bahl, M.-O., Matsubara, S., Huesgen, P.F., 2020. Photoprotective acclimation of the *Arabidopsis thaliana* leaf proteome to fluctuating light. Front. Genet. 11, 154. https://doi: 10.3389/fgene.2020.00154

Poorter, H., Niinemets, Ü., Ntagkas, N., Siebenkäs, A., Mäenpää, M., Matsubara, S., Pons, T.L., 2019. A meta-analysis of plant responses to light intensity for 70 traits ranging from molecules to whole plant performance. New Phytol. 223(3), 1073-1105. https://doi.org/ 10.1111/nph.15754.

Rantala, M., Rantala, S., Aro, E.-M., 2020. Composition, phosphorylation and dynamic organization of photosynthetic protein complexes in plant thylakoid membrane. Photochem. Photobiol. Sci. https://doi.org/10.1039/d0pp00025f

Rassadina, V.V., Averina, N.G., Koval, S.F., 2005. Disturbance of chlorophyll formation at the level of 5-aminolevulinic acid and Mg-containing porphyrin synthesis in isogenic lines of spring wheat (*Triticum aestivum* L.) marked with genes *cn-A1* and *cn-D1*. Dokl. Biol. Sci. 405, 472–473. https://doi.org/10.1007/s10630-005-0169-8

Ruban, A.V., 2016. Nonphotochemical chlorophyll fluorescence quenching: mechanism and effectiveness in protecting plants from photodamage. Plant Physiol. 170(4), 1903-16. https://doi.org/ 10.1104/pp.15.01935.

Sacksteder, C.A., Kramer, D.M., 2000. Dark interval relaxation kinetics of absorbance changes as a quantitative probe of steady-state electron transfer. Photosynth. Res. 66, 145–158. https://doi.org/10.1023/A:1010785912271

Salter, W.T., Merchant, A.M., Richards, R.A., Trethowan, R., Buckley, T.N., 2019. Rate of photosynthetic induction in fluctuating light varies widely among genotypes of wheat. J. Exp. Bot. 70, 2787-2796.

Schneider, T., Bolger, A., Zeier, J., Preiskowski, S., Benes, V., Trenkamp, S., Usadel, B., Farré, E.M., Matsubara, S., 2019. Fluctuating light interacts with time of day and leaf development stage to reprogram gene expression. Plant Physiol. 179, 1632-1657.

Schumann, T., Paul, S., Melzer, M., Dörmann, P., Jahns, P., 2017. Plant growth under natural light conditions provides highly flexible short-term acclimation properties toward high light stress. Front. Plant Sci. 8, 681.

Shimakawa, G., Miyake, C., 2018a. Oxidation of P700 ensures robust photosynthesis. Front. Plant Sci. 9, 1617. https://doi.org/10.3389/fpls.2018.01617.

Shimakawa, G., Miyake, C., 2018b. Changing frequency of fluctuating light reveals the molecular mechanism for P700 oxidation in plant leaves. Plant Direct 2, e00073. https://doi.org/10.1002/pld3.73.

Slattery, R.A., Walker, B.J., Weber, A.P.M., Ort, D.R., 2018. The impacts of fluctuating light on crop performance. Plant Physiol. 176, 990-1003. https://doi.org/10.1104/pp.17.01234

Song, Q., Wang, Y., Qu, M., Ort, D.R., Zhu, X.G., 2017. The impact of modifying photosystem antenna size on canopy photosynthetic efficiency-development of a new canopy photosynthesis model scaling from metabolism to canopy level processes. Plant Cell Environ. 40, 2946–2957. https://doi.org/10.1111/pce.13041

Sukhov, V., Surova, L., Sherstneva, O., Katicheva, L., Vodeenev, V., 2015. Variation potential influence on photosynthetic cyclic electron flow in pea. Front. Plant Sci. 5, 766. https://doi.org/10.3389/fpls.2014.00766.

Suorsa, M., Järvi, S., Grieco, M., Nurmi, M., Pietrzykowska, M., Rantala, M., Kangasjärvi, S., Paakkarinen, V., Tikkanen, M., Jansson, S., Aro, E.-M., 2012. PROTON GRADIENT REGULATION5 is essential for proper acclimation of *Arabidopsis* photosystem I to naturally and artificially fluctuating light conditions. Plant Cell 24(7), 2934-48. https://doi.org/10.1105/tpc.112.097162.

Tanaka, Y., Adachi, S., Yamori, W., 2019. Natural genetic variation of the photosynthetic induction response to fluctuating light environment. Curr. Opin. Plant Biol. 49, 52-59. https://doi.org/10.1016/j.pbi.2019.04.010

Takizawa, K., Cruz, J.A., Kanazawa, A., Kramer, D.M., 2007. The thylakoid proton motive force in vivo. Quantitative, non-invasive probes, energetics, and regulatory consequences of light induced *pmf*. Biochim. Biophys. Acta 1767, 1233–1244. https://doi.org/10.1016/j.bbabio.2007.07.006

Tikkanen, M., Grieco, M., Nurmi, M., Rantala, M., Suorsa, M., Aro, E.-M., 2012. Regulation of the photosynthetic apparatus under fluctuating growth light. Phil. Trans. R. Soc. B 367, 3486–3493. https://doi.org/10.1098/rstb.2012.0067

Trissl, H., 1997. Determination of the quenching efficiency of the oxidized primary donor of Photosystem I, $P700^+$: implications for the trapping mechanism. Photosynth. Res. 54: 237–240. https://doi.org/10.1023/A:1005981016835

van Bezouw, R.F.H.M., Keurentjes, J.J.B., Harbinson, J., Aarts, M.G.M., 2019. Converging phenomics and genomics to study natural variation in plant photosynthetic efficiency. Plant J. 97, 112–133. https://doi.org/10.1111/tpj.14190

Vialet-Chabrand, S., Matthews, J.S., Simkin, A.J., Raines, C.A., Lawson, T., 2017. Importance of fluctuations in light on plant photosynthetic acclimation. Plant Physiol. 173(4), 2163-2179. https://doi.org/10.1104/pp.16.01767.

Wang, Y., Zheng, W., Zheng, W., Zhu, J., Liu, Z., Qin, J., Li, H., 2018. Physiological and transcriptomic analyses of a yellow-green mutant with high photosynthetic efficiency in wheat (*Triticum aestivum* L.). Funct. Integr. Genomics 18, 175–194. https://doi.org/10.1007/s10142-017-0583-7

Watanabe, N., Koval, S.F., 2003. Mapping of chlorina mutant genes on the long arm of homoeologous group 7 chromosomes in common wheat with partial deletion lines. Euphytica 129, 259–265. https://doi.org/10.1023/A:1022276724354

Wientjes, E., van Amerongen, H., Croce, R., 2013. LHCII is an antenna of both photosystems after long-term acclimation. Biochim. Biophys. Acta 1827(3), 420-6. https://doi.org/ 10.1016/j.bbabio.2012.12.009.

Yamori, W., 2016. Photosynthetic response to fluctuating environments and photoprotective strategies under abiotic stress. J. Plant Res. 129(3), 379-95. https://doi.org/ 10.1007/s10265-016-0816-1.

Yin, X., Struik, P.C., Romero, P., Harbinson, J., Evers, J.B., van der Putten, P.E.J., Vos, J., 2009. Using combined measurements of gas exchange and chlorophyll fluorescence to estimate parameters of a biochemical C3 photosynthesis model: a critical appraisal and a new integrated approach applied to leaves in a wheat (*Triticum aestivum*) canopy. Plant Cell Env. 32, 448-464. https://doi.org/10.1111/j.1365-3040.2009.01934.x

Yokono, M., Takabayashi, A., Akimoto, S., Tanaka, A., 2015. A megacomplex composed of both photosystem reaction centres in higher plants. Nat. Commun. 6, 6675. https://doi.org/ 10.1038/ncomms7675.

Yokono, M., Akimoto, S., 2018. Energy transfer and distribution in photosystem super/megacomplexes of plants. Curr. Opin. Biotech. 54, 54-56. https://doi.org/10.1016/j.copbio.2018.01.001

Živčak, M., Brestič, M., Balatova, Z., Drevenakova, P., Olsovska, K., Kalaji, H.M., Yang, X., Allakhverdiev. S.I., 2013. Photosynthetic electron transport and specific photoprotective responses in wheat leaves under drought stress. Photosynth. Res. 117(1-3), 529-546. https://doi.org/ 10.1007/s11120-013-9885-3.

Živčak, M., Brestič, M., Kalaji, H.M., Govindjee, 2014. Photosynthetic responses of sun- and shade-grown barley leaves to high light: is the lower PSII connectivity in shade leaves associated with protection against excess of light? Photosynth. Res. 119(3), 339-354. https://doi.org/10.1007/s11120-014-9969-8.

Živčak, M., Brestič, M., Botyanszka, L., Chen, Y.E., Allakhverdiev, S.I., 2019. Phenotyping of isogenic chlorophyll-less bread and durum wheat mutant lines in relation to photoprotection and photosynthetic capacity. Photosynth. Res. 139(1-3), 239-251. https://doi.org/ 10.1007/s11120-018-0559-z.